Tutor

Prof. Fidel Cunill García
Departament d'Enginyeria Química

Grau en
Enginyeria
Química

Treball Final de Grau

Contribución al estudio de la síntesis de butil levulinato en fase líquida sobre resinas de intercambio iónico.

A contribution to the study of butyl levulinate synthesis in the liquid-phase on ion-exchange resins.

M. Àngels Tejero Iborra

June 2015

Universitat
de Barcelona

Dos campus d'excel·lència internacional

B:KC Barcelona Knowledge Campus   HUB Health Universitat de Barcelona Campus

If we knew what it was we were doing, it would not be called research, would it?

Albert Einstein

Als meus pares, per el seu suport i per la incondicional fe i confiança en les meves habilitats que han demostrat sempre. Als meus professors, a tots ells sense excepció, perquè a més de complir amb la seva encomiable labor docent m'han ensenyat el valor de la dedicació i l'esforç. A en Dr. Roger Bringué per la seva desinteressada ajuda en els meus primers dies davant d'un instal·lació. A en Rodrigo Soto i Jordi Hug Badía per haver-me escoltat amb paciència i la seva actitud comprensiva. I a tot el grup de Cinètica i Catàlisi Aplicada, per el seu suport col·lectiu.

Gràcies.

REPORT

CONTENTS

1. SUMMARY

Alkyl levulinates are biomass derived chemicals with a large spectrum of applications. They have the potential to substitute compounds currently derived from petro-chemical routes as components of conventional diesel or gasoline because of their physicochemical properties. Alkyl levulinates are synthesized most often from levulinic acid, but also from furfuryl alcohol or directly from cellulose and monosaccharide sugars. Levulinic acid is a platform chemical formed from hydrolysis of lignocellulose, the most readily available form of biomass, using the Biofine process.

The most widely studied alkyl levulinate is ethyl levulinate, both its synthesis pathways and possible applications have been explored thoroughly. Comparatively, the potential of butyl levulinate has been left untapped. As an additive for automotive diesel fuel, butyl levulinate is even more promising than ethyl levulinate: butyl levulinate remains in diesel solution down to the diesel cloud point; butyl levulinate blends have very small particulate matter emissions; it has a lower solubility in water than ethyl levulinate; good lubricity and conductivity; and a low but better cetane number.

Esterification of levulinic acid with butanol over several types of catalysts such as zeolites, lipases and heteropolyacids (HPA) supported on acid-treated clay montmorillonite (K10) has been described in literature, but the catalysis with acidic ion-exchange resins has never been attempted to the best of our knowledge. The present work studies the behavior of different sulfonated polystyrene-divinylbenzene resins in the synthesis of butyl levulinate from levulinic acid.

The conducted experiments confirm that acidic polymer catalysts can be used in order to obtain very high conversion and selectivity in the esterification of levulinic acid with butanol to butyl levulinate. Selectivity toward butyl levulinate remains always over 98% for all tested catalysts in the range of temperatures studied, and the most relevant by-product is dibutyl ether. The catalyst with highest activity was Dowex 50Wx2, and overall, gel-type resins presented

better yields than macroporous ones. Because of the high polarity of levulinic acid and the formation of water, resins with greater capacity for swelling would favor levulinic acid esterification. Thus resins with a lesser degree of cross-linking present higher reaction rates.Globally, reaction rates improve as the degree of polymer cross-linking diminishes and roughly correspond with large specific volume of swollen polymer.

2. RESUM

Els alquil levulinats son substàncies químiques derivades de la biomassa amb un ampli espectre d'aplicació. Tenen el potencial per a substituir compostos químics que actualment deriven de rutes petroquímiques, tals com components de combustibles diesels convencionals o gasolines, degut a les seves propietats fisicoquímiques. Els alquil levulinats es sintetitzen normalment a partir de l'àcid levulinic, però també partint de l'alcohol furfurílic, o directament a partir de la cel·lulosa o monosacàrids. L'àcid levulinic, es una molècula plataforma formada mitjançant la hidròlisi de la lignocel·lulosa, la biomassa més fàcilment accessible, per el procés Biofine.

L'alquil levulinat més exhaustivament estudiat és l'etil levulinat, tant pel que fa a les seves possibles rutes de síntesi com a les seves possibles aplicacions. Comparativament, el potencial del butil levulinat ha estat completament ignorat. Com a additiu per a combustibles diesel per a l'automoció el butil levulinat es encara més prometedor que l'etil levulinat. El butil levulinat es manté en solució dins del diesel fins al punt d'enboirament (*cloudpoint*)d'aquest, mescles amb diesel produeixen molt poques emissions de partícules, la seva solubilitat en aigua es menor que la de l'etil levulinat, té bona lubricitat i conductivitat i un nombre de cetà baix, encara que superior al de l'etil levulinat.

L'esterificació de l'àcid levulinic amb butanol ha estat descrita en la literatura mitjançant l'ús de catalitzadors com les zeolites, lipases i heteropoliàcids (HPA) suportats sobre argila montmorillonítica tractada amb àcid (K10). Tanmateix la catàlisis d'aquesta reacció mitjançant resines de bescanvi iònic no s'ha dut mai a terme segons els nostres registres. El present treball estudia el comportament de diferent resines de poliestirè-divinilbenzè sulfonades en la síntesi de butil levulinat a partir de l'àcid levulinic.

Els experiments duts a terme demostren que catalitzadors polimèrics àcids poden ser emprats per tal d'obtenir conversions i selectivitats molt elevades en l'esterificació de l'àcid levulínic amb butanol per tal d'obtenir butil levulinat. La selectivitat a favor del butil levulinat és sempre superior al 98% per a totes les resines en el rang de temperatures estudiat, mentre que

el producte secundari més rellevant és el dibutiléter. El catalitzador amb una activitat més elevada ha resultat la resina Dowex 50Wx2, i de forma global, les resines tipus gel han presentat conversions superior a les resines macroporoses. Degut a la elevada polaritat de l'àcid levulínic i la formació d'aigua durant el transcurs de la reacció, els catalitzadors que presenten un inflament de la matriu polimèrica més pronunciat afavoreixen l'esterificació de l'àcid levulínic. Per tant, resines amb un grau de reticulació menor presenten velocitats de reacció més elevades. En conjunt, les velocitats de reacció es veuen afavorides per una disminució en el grau de reticulació i es corresponen amb elevats volums específics de polímer inflat.

3. INTRODUCTION

3.1. FROM BIOMASS TO BIOFUELS

In the last few decades the need of society to reduce its dependence on imported crude oil has been directing researchers attention to the use of biomass as a source of renewable energy and replacing existing products directly derived from petrochemical routes. Biomass provides an ideal alternative to fossil resources because it is the only sustainable source of organic compounds[1].

The term biofuel is referred to biomass-to-liquid fuels (BTL). Liquid biofuels offer a promising alternative as substitute fuels sources to petroleum, however most still contain significant amounts of petroleum in the mixture. The liquid biofuels most widely used currently are biodiesel (obtained by transesterification of triglycerides with methanol or ethanol to a lesser degree) and bioethanol (from fermentation of edible biomass sources). They are extensively produced and consumed mainly because their production is based on simple and well-known technologies, and are usually used blended with conventional fuels. The biggest difference between this first-generation biofuels and petroleum feedstocks is oxygen content, which has the advantage of a cleaner combustion but also presents several drawbacks: it imparts a lower energy content, poor thermal stability, lower volatility, higher corrosivity and a tendency to polymerize over time[2-3]. Additionally they are produced from classic food crops that require high-quality agricultural land for growth. The world faces serious food-supply problems. Our society faces the dilemma of diverting farmland and crops towards the production of liquid biofuels in detriment of the food supply on a global scale. First-generation biofuels appear unsustainable because of the potential stress their production places on food commodities [2]. Hence, there has been a focus on developing commercially viable technologies for the production of biofuels compatible with existing vehicle engines and fuel infrastructure that do not require feedstocks from food crops and can overcome most of the current drawbacks for their use as transportation fuels. Yet there are important obstacles to all proposed alternatives which

have prevented commercial second generation biofuels (which are derived from non-food crops) from being produced to date[4].

The simplest answer as to why commercial scale biorefineries are not operational is that they are not currently cost competitive with first generation biofuels and fossil fuels, even given the extra financial incentives that may be in place in different countries. The process of releasing the sugars from their lignocelullosic matrix economically and in high yields has been more difficult than initially expected. It has been estimated that this stage can contribute 40–45% to the total biofuel cost [5]. Many of the problems associated with achieving high sugar yields in a cost-effective manner are related to the complex macrostructure of the lignocellulosic matrix. Given the recalcitrance of lignocellulose, it is very important that pretreatments are carried out prior to hydrolysis, and this stage is one of the current limiting factors in allowing for cost-effective second generation biofuels. The following conversion of the sugars liberated in hydrolysis is equally problematic. Whether through fermentation into ethanol by the use of microorganisms or the degradation into other more attractive products, depend to a large extent on whether high yields can be achieved in a cost-effective manner.

However, the commercial scale production of liquid hydrocarbons from biomass is getting near. There has been important work in order to improve existing processes with genetically altered microorganisms by companies such as Amyris and LS9 [1]and a process known as Bioforming was developed by Virent Energy Systems that converts water-soluble sugars into green gasoline, diesel and jet fuel[6]. Pyrolysis efforts are led by UOP and Ensyn[7], and KiOR attempted to develop a biomass catalytic cracking process analogous to catalytic cracking of petroleum refineries[8]. Meanwhile, Choren Industries in Germany is in the process of commercializing a biomass-to-liquids operation based on gasification.

Vegetable biomass (mainly lignocellulose) is composed of lignin (15-20%), hemicellulose (25-35%) and cellulose (40-50%). Lignin is a highly cross-linked polymer built of substituted phenols with a rigid three-dimensional structure responsible for the structural integrity of plants. Hemicellulose is a polymer formed by C6 and C5 sugar monomers, and cellulose is a polymer of glucose units. Most technical approaches to converting lignocellulosic material into chemicals and fuels have been geared towards liberating cellulose from its lignin supports and breaking down its rigid structure so the cellulose can be hydrolyzed into glucose monomers. Besides these components, plants also elaborate energy storage products such as lipids, sugars,

starches and terpenes. If one considers the energy contents of biomass products, terpenes are at the top of the list, followed by vegetable oils, lignin and sugars [9].

Biomass can be used as a raw material to produce a large number of chemicals with the potential to be fundamental to the chemical industry as platform chemicals or building blocks. To date, many of these products have failed in the marketplace because they are not yet available at a low enough cost. The conversion of vegetable feedstocks into valuable products is a set of subsequent transformations of staple biomass-derived molecules known as platform chemicals. The three main routes to transform biomass into fuels and chemicals are gasification, pyrolysis and hydrolysis. Hydrolysis is the more complicated process and requires that lignocellulose be broken into its constituent parts. The transformation of hydrolysis-obtained sugars into bioproducts can take place through either fermentation processes or other chemical transformation in biorefineries.
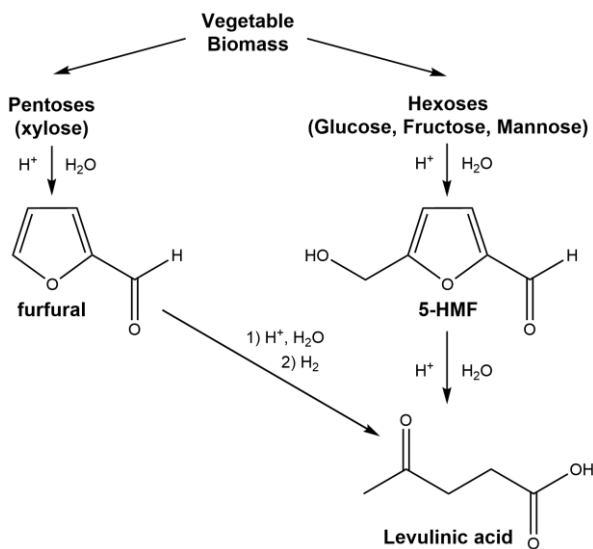
Figure 1. Products obtained by dehydration of monosacharides.

The chemical transformation of monosaccharides (glucose, fructose and xylose) is done mainly through thermal dehydration in acid media, which leads to three important platform chemicals: furfural, 5-hydroxymethyl-furfural (HMF) and levulinic acid (Figure 1).

Levulinic acid (LA, 4-oxopentanoic acid) was highlighted by the United States Department of Energy as a promising building block for chemistry in 2004 and 2010. It can be considered one

of the most important platform molecules derived from biomass because of its reactive nature along with the fact that it can be produced now from lignocellulosic waste at low cost.

LA has been produced since 1870. Its acid properties and chemistry were studied extensively. Yet, despite having a lot of potential as an industrial chemical, commercial use at any significant level failed to materialize until the last two decades[10]. This has been attributed to the fact that most of the early research was done at a time (1940s) in which corresponding raw materials were expensive, reaction yield was low and equipment for its purification and separation were still lacking. It was not until the Biofine Process became operational in 1996 that there was a reevaluation of LA's industrial potential[11-12]. The Biofine Process is one of the most advanced and commercially viable lignocellulosic-fractionating technologies currently available, producing LA from cellulosic feedstocks including wood waste and agricultural residues. LA and its derivatives are used in a good number of different industrial applications.

Key industry participants such as DuPont, Segetis and Biofine have already developed patented technologies for levulinic acid commercialization through renewable sources. Currently LA costs between 5 to 8 USD per kilo, which is somewhat high for a prospective platform chemical. Nonetheless, prices can be expected to drop with a target price of less than USD 1 per kilo once the relevant conversion technologies have been successfully commercialized[13]. It is expected that the reduced price will open a host of opportunities including energy, transportation, green chemicals and specialty polymers [14].

LA and a number of derivatives have been proposed as green solvents[15], and specifically as a solvent for aromatic constituents of mineral oil. It is also a platform chemical from which other more valuable intermediates are derived in the synthesis of polymers such as synthetic rubber from piperylene[16] or other alkyd resins from biphenolic acid [17]which have potential application as adhesives. LA is regularly applied to the food industry as an acidulant in carbonated and fruit juice beverages, jams and jellies. Finally, sodium and calcium salts of LA have been found to have therapeutic uses as well as a potential application as a substitute of ethylene glycol in antifreeze [10]. Levulinic acid also acts as a potential replacement to phthalate plasticizer added to manufacture PVC, the largest consumed commodity plastic [14].

Esters of levulinic acid are the most notable LA derivatives that could potentially be used as fuel liquid extenders and because of this they are possibly the most interesting.

3.2. SYNTHESIS OF ALKYL LEVULINATES AND THEIR APPLICATION AS BIOFUELS

Alkyl levulinates are biomass derived chemicals with a large spectrum of applications. They are used as solvents because they are all soluble in classical solvents (alcohols, ethers and chloroform) [15]. Their use has been patented for mineral oil refining [18]. LA esters have a wide range of application as additives to polymers, perfume, flavoring preparations and latex coating compositions [19-21].They have the potential to substitute compounds currently derived from petro-chemical routes as additives to conventional diesel or gasoline because of their low toxicity and physicochemical properties; exhibiting characteristics that make them appropriate for use as cold-flow improvers in biodiesel or oxygenate additives for gasoline and diesel fuel. Alkyl levulinates are synthesized most often from levulinic acid (LA), but also from furfuryl alcohol or directly from cellulose and sugars [22].
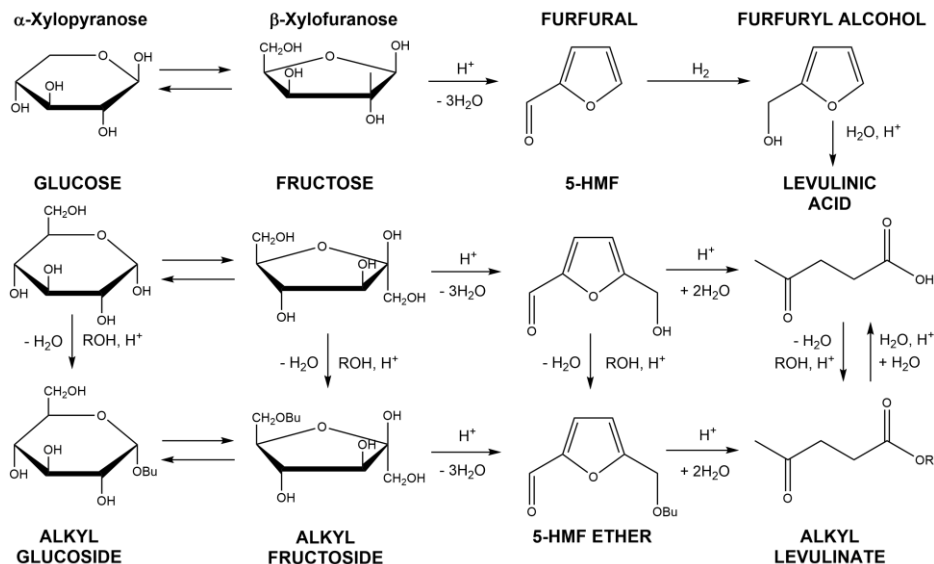
Figure 2. Main synthesis routes for alkyl levulinates.

Levulinate esters can be obtained through different routes (Figure 2). One of them is direct esterification of levulinic acid with alcohols, typically acid catalyzed. Alkyl levulinates were first synthesized by Sah[23], and later Schuette[24] and Cox[25] by this method, publishing the formation of a number of alkyl levulinates in the corresponding alcohol in the presence of HCl. In these early studies yields were reportedly low (35-75%) and relatively high temperatures (110-162ºC).

Although comparison is difficult due to very different experimental conditions, some general trends can be outlined. Typically a solvolysis, the alcohol itself always acts as a solvent and thus is always in excess. Nonetheless, the molar ratio of alcohol to LA falls often in the 5-10 range. This ratio is low enough for the alcohol dehydration that leads to the formation of symmetrical ethers to be somewhat prevented. As esterification is a reversible reaction, excessive alcohol is favorable to ester formation. However, much more alcohol may dilute the reactant, thereby creating mass transfer limitations between the reactants to the solid catalysts [22]. Temperatures typically range between 65 and 160ºC depending on the alcohol used for esterification and the catalyst employed in the levulinate synthesis.

The early studies used mostly homogeneous catalysis, but more recently a variety of heterogeneous catalysts have been tested. Heterogeneously catalyzed esterification of LA uses most often solid Brønsted acids. It has been proposed that the mechanism for the esterification of LA on acidic surfaces involves the adsorption through the protonated carbonyl group (carboxyl group) enabling a nucleophilic attack of the alcohol assisted by an oxygen atom from the catalyst structure [26-27].

The most widely studied alkyl levulinate is ethyl levulinate (EL), both its synthesis pathways and possible applications have been explored thoroughly. Traditionally EL was synthesized by using homogeneous catalysts such as HCl, H_3PO_4 and H_2SO_4. These inorganic liquid acids cause environmental problems in disposal, containment and handling due to their toxic and corrosive nature. Very recently, this reaction has been re-examined extensively with more robust and industrially benign greener catalysts. For this purpose have been studied eco-friendly solid acid catalysts including supported heteropoly acids HPA[26-29], zeolites[27,30], hybrid catalysts[31-33], sulfated carbon nanotubes[34], Starbon® mesoporous materials functionalised with sulfonated groups[35], sulfated metal oxides[32] and silicas[36-37] and immobilized lipases[38]. It has also been synthesized using commercial PS-DVB acidic sulfonic resins as baseline reference catalysts, usually Amberlyst 15 [27-28, 34, 36]. At the same time there have been steps taken towards perfecting the conversion of lignocellulose, glucose or fructose directly into ethyl levulinate ina one-step process catalyzed either by H_2SO_4 or ZrO_2-based sulfonated catalysts [39-42].

But what makes a good biofuel candidate? All automotive fuels must meet a minimum performance requirements set by different countries, generally developed with functional vehicle

engine performance in mind. Similarly, when blended with conventional diesel fuel and gasoline they must remain in compliance with laws that have been implemented in order to guarantee that they do not contribute to the failure or deterioration of any emission control devices and produce low atmospheric emissions (SO_2 in exhaust gases and combustion fumes). Also it is required that its melting point should be well below ambience temperature particularly in winter. Butmost importantly, automotive fuels must provide an adequate burn rate in the conditions present inside the engine: neither too fast (in order to prevent overheating to the injector) nor too slow (in which case fuel would reach the cylinder's walls without burning).The quality of European diesel fuels is specified by the EN 590 standard (Directive 2009/30/EC). While these specifications are not mandatory, they are observed by all fuel suppliers in Europe (Table 1).

Fuel property	Unit	Specification		Test
		Min	Max	
Cetane Number	-	51	-	ISO 5165
Cetane Index	-	46	-	ISO 4264
Density (15ºC)	kg/m³	820	860	ISO 3675 / ASTM D4052
Sulfur	ppm	-	50	EN 24260 / ISO 8754
Flash Point	ºC	55	-	ISO 2719
Carbon residue (10%btms)	% (wt.)	-	0.30a	ISO 10370
Ash	% (wt.)	-	0.01	EN 26245
Water content	mg/kg	-	200	ASTM D1744
Copper strip corrosion, 3h (50ºC)	-	-	Class 1	ISO 2160
Oxidation stability	g/m³	-	25	ASTM D2247
Viscosity (40ºC)	mm²/s	2.00	4.50	ISO 3104
Distillation (vol. % recovered)	ºC			IS 3405
10% point	ºC	report	-	
50% point	ºC	report	-	
65% point	ºC	250	-	
85% point	ºC	-	350	
95% point	ºC	-	370	
FAME content	% (wt.)	7	-	

(a) limit does not apply if ignition improver additives are used

Table 1. EN 590:2009 Diesel Fuel Specification.

Cetane number is a measure of the ignition delay of a diesel fuel [43]. The higher the cetane number, the shorter the interval between the time the fuel is injected and the time it begins to burn. It is a measure of the ease with which the fuel can be ignited and is most significant in low temperature starting, warm up, idling and smooth, even combustion. Some hydrocarbons ignite

more readily than others and are desirable because of this short ignition delay. Low cetane number usually causes an ignition delay in the engine, poor fuel economy, a loss of power and sometimes engine damage.

A minimum value for *density* guarantees that the engine will have sufficient power, while an excess might lead to smoke production. Viscosity provides information regarding circulation and lubricity. *Sulfur content* must be as low as possible because it can contribute significantly to particle and SO_2 emissions. However, some processes used to desulphurize diesel fuel reduce its natural lubricating qualities. Since diesel fuel must have sufficient lubricity to give adequate protection against excessive injection system wear other components are added to diesel fuels to palliate this effect.

Volatility characteristics are very specific because it must be adequate for high pressure injection and facilitate the atomization by spraying. For this reason, the distillation curve must meet the specifics in distilled fraction volume percentage (Table 1).

If diesel fuel is cooled, it will eventually reach its *cloud point*. This is the temperature at which fuel will lose transparency due to the wax paraffin crystallization. The temperature at which fuel will no longer flow or turns solid is known as the pour point. Another key property of diesel fuel is the *cold filter plug point*, which is the temperature where fuel can no longer flow freely through a fuel filter, approximately halfway between the cloud point and the pour point. The flash point is the minimum temperature at which fuel must be heated in order to liberate vapors that ignite in contact with air or a flame.

One of the more common contaminants in fuel is water. Water can cause injector nozzle and pump corrosion, bacteria and fungi growth and fuel filter plugging. It is thus considered appropriate that all automotive fuels have very low miscibility in water. *Carbon residue* gives a measure of the carbon depositing tendencies of a diesel fuel after evaporation and pyrolysis under prescribed conditions. While not directly correlating with engines deposits, this property is considered a guide. Ash forming material may be present in diesel fuel as abrasive solids which contribute to injector, fuel pump, piston and ring wear, and also engine deposits. If a diesel fuels corrosive tendencies are not controlled the possibility of corrosion to copper, brass or bronze parts in the fuel system may occur. This is tested by *copper strip corrosion*.

As a fuel liquid extender, EL has been considered often in recent years. This is because relative to ethanol, blends with gasoline of cellulose derived oxygenates (such as EL) could

potentially have higher energy density, lower vapor pressure and less affinity for water[44]. EL was investigated as a novel, bio-based cold flow improver for use in biodiesel fuels[45]. It was concluded that blending EL improved the low temperature properties of biodiesel.

Comparatively, the potential of butyl levulinate (BL) has been left untapped. A 2011 study assessed both EL and BL as diesel blend components[46]. As an additive for diesel, BL is also promising. Both EL and BL reduce vapor pressure in diesel blends [44]. The freezing point of both esters is below -60ºC, and their boiling point and flash point are in the acceptable range for diesel fuel. Remarkably though, BL is only sparingly soluble in water unlike EL (El is soluble up to 15.6 wt% and BL only 1.3 wt%). Although they both exhibit less energy per volume than conventional diesel fuel with 31% (EL) and 25% (BL) less, this is already an improvement on bioethanol. In mixtures of 20% levulinate blends, EL tends to form a separate liquid phase in most diesel fuels at temperatures significantly above the cloud point of diesel fuel. BLremains completely soluble in diesel down to the diesel cloud point (around -25.8ºC). Addition to diesel fuel had no effect on total hydrocarbon, carbon monoxide or particulate matter emissions. Furthermore high-content BL-diesel blending (20 wt% BL) showed that engine out-smoke was reduced by 55% and virtually free-soot combustion. Both esters improved the lubricity and conductivity of the diesel fuel into which they were blended. Nonetheless both esters exhibit a very low cetane number (although BL less so), which means blending with these components requires cetane-enhancing additives.

Thus while it appears that EL is a more adequate gasoline additive, BL is to all appearances more appropriate for diesel blending. Additionally butanol, like ethanol can be synthesized from renewable crop resources. Yet despite being potentially better as a diesel fuel additive, BL synthesis has been mostly overlooked. Like all alkyl levulinate first attempts at synthesis were undertaken with homogeneous catalysis in the early 1930s [23-25]. Additionally a kinetic model for the esterification of LA with butanol (BuOH) was proposed by Bart et al.[47].Some work has been made in BL production directly from cellulose with homogeneous catalysis [48].

Esterification of LA with butanol over several types of solid catalysts such as zeolites [49], and heteropolyacid (HPA) supported on acid-treated clay montmorillonite (K10) [50]has been described in literature since then. There have also been sporadic but successful attempts at production and kinetic modelling of BL by esterification of LA via immobilized lipase catalysis [51].

Surprisingly the catalysis with acidic ion-exchange resins has never been attempted to the best of our knowledge.
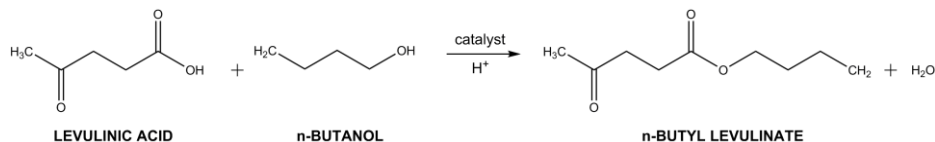
Ref.	Catalyst	Solvent	Catalyst load	t (h)	T (ºC)	$R_{BUTOH/LA}$	X_{LA} (%)
[49]	Zeolite	None (BuOH)	7-14 wt%	4-12	120	6-8	82
[50]	HPA on K10	None (BuOH)	7-30 wt%	1-6	120	4-10	97
[51]	Immobilized lipase	t-butyl methyl ether	10-50 mg	2	30-60	1-4	88

Table 2. Summary of experimental conditions used in synthesis of BL by heterogeneous catalysis.

3.3. ACIDIC ION-EXCHANGE RESINS OF POLYSTYRENE-DIVINYLBENZENE (PS-DVB) AS CATALYSTS

Heterogeneous catalysis is the kind most common in industrial processes, mostly because they present fewer problems from an engineering standpoint. Approximately 80% of industrial catalytic processes use heterogeneous catalysis and of those, 90% are catalyzed by solids[52].

At least one of the reagents must interact with a solid's surface and be adsorbed in order for a solid to act as catalyst. Having a large and extensive surface where the reactants can be adsorbed is essential. Therefore most heterogeneous catalysts are porous solids, which feature a large surface area in a small volume. The structure of solid catalyst particles (number, size and pore volume) is fundamental in catalyst performance. A typical catalyst contains one or more groups of pores (pore structure), which size and volume depend on preparation method. Their chemical composition is also important because the interaction of the reactants with the surface is of a chemical nature[52]. The different chemical stages of a solid catalyzed reaction (reagents adsorption, reaction and product desorption) take place in specific places in the catalyst surface called active sites.

The interest of a solid catalyst is always assessed in terms of activity (measured in conversion), selectivity, lifespan and reusability. Typically heterogeneous catalysts can be metals, metallic oxides, metallic salts, non-metallic oxides, zeolites (silica and/or alumina oxides) or functionalized ion-exchange resins.

Ion-exchange resins are functionalized polymeric materials capable of exchanging ions with the medium in which they are immersed. They present numerous advantages such as being insoluble, mechanically and relatively thermally stable. A catalytic resin consists of an insoluble matrix in which functional groups are anchored. The polymer matrix is made of long hydrocarbon chains structured by means of a cross-linking agent. The cross-linking agent confers the matrix with a stable tridimensional hydrophobic structure and a defined pore structure. Pores are classified depending on their size: ultramicropores (size < 0.7nm), micropores (size < 2nm), mesopores (2nm < size < 50nm) and macropores (size > 50nm) [53]. The polymer matrix contains the functional groups responsible for its acidity, basicity or even both depending on their specific nature. The specific properties of a resin are determined not only by the matrix and functional groups, but also by the polymer structure which is the result of the synthesis methods employed. The thermal and mechanical resistance of these catalysts depends essentially on the degree of cross-linking and the nature of its functional groups.

There are a great many advantages of the use of ion-exchange resins. There is the ease of handling and storage. Corrosion problems can be avoided because most protons are on the inside of catalyst particles and waste treatment is much simplified by the reduced acidity or basicity of waste products. They are equally appropriate for work in continuous and batch reactors and thus inherently flexible. Because their density is very similar to the most common organic solvents they can easily remain in suspension even at low stirring speeds. They are easily separated from reaction mixtures by filtering, which leads to higher purity products and yields. This simplifies industrial processes by doing away with several separation steps and units, which has a great impact in cost. These catalysts are of acceptable duration and the possibility of regeneration always exists, reducing the cost of catalysts used, even if they are already inexpensive. Additionally obtaining water-free products is easier because these resins can work even in completely non-polar media.

Widely used amongst a vast variety of different ion-exchange resins are those with styrene-divinylbenzene (PS-DVB) matrixes (Figure 3). These resins are obtained by polymerization of styrene and the subsequent addition of a specific amount of divinylbenzene. This produces the aforementioned tridimensional and insoluble structure. On cue, these resins are sulfonated by means of a concentrated sulfuric acid bath in order for them to acquire their acid properties. Depending on the specifics of their synthesis, acidic ion-exchange resins present different

structures with varying degrees of cross-linking, swelling, particle diameter, acid capacity, density, affinity to water and stability.
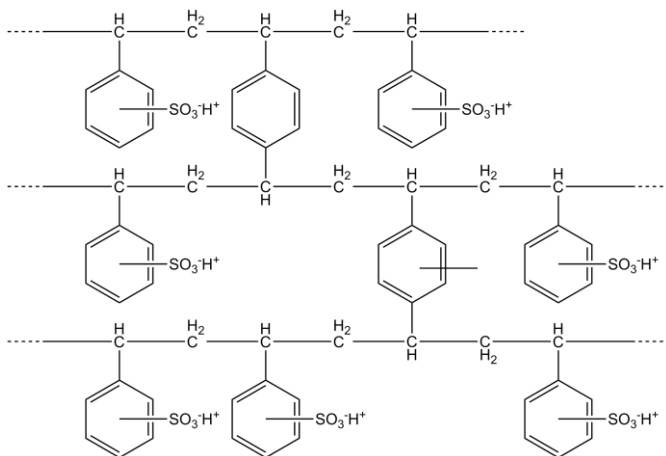
Figure 3.Structure of a sulfonated resin of PS-DVB.

After the polymerization of PS-DVB, particle diameter usually has a Gaussian distribution that is characterized by sieving into different fraction with different mesh sizes. For the most part, commercially used resins have particle diameters comprised between 0.21 and 1.20 mm. Shape and size allow these materials to be easily and quantitatively recovered by simple filtration or decantation. This is not the case for other powdered materials often used as catalysts support (e.g., silica, zeolites, carbon, etc.) [54].

The cross-linking degree relates to the proportion (weight %) of reticulating agent (DVB) present in the initial monomer solution before the polymerization reaction takes place (typically from 0.5 to 25wt%) [54]. It is the variable that controls resin porosity. Porosity in turn, affects some bulk properties of the resins which have consequences on their catalytic applications, i.e. swelling, acid capacity and selectivity. Usually, the lower the cross-linking percentage, the higher the moisture content and the ability to accommodate larger molecules.A high cross-linking degree provides greater strength and stiffness to resins. Highly cross-linked resins are more likely to withstand oxidizing conditions, but often are more brittle. Furthermore, a high degree of cross-linking leads to internal mass transference problems arising from the very dense structure they present. On the other hand, low cross-linking leads to soft, elastic and mechanically unstable resins.
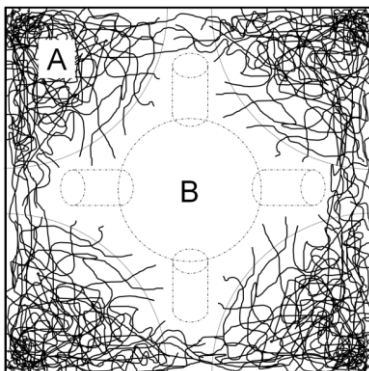
Figure 4. Morphology of a macroreticular resin: A) gel-phase area. B) macropores.

Low cross-linked resins (gel-type) have a microporous structure, whereas higher cross-linkage degrees result in macroreticular (macroporous) resins. Because of the low amounts of cross-linking agent, gel-type resins have a reduced surface area (<1m^2/g) while dry with a pore structure is comprised of micropores between 7 and 15 Å. These are not permanent pores, but they appear in the presence of polar solvents when the resins experience a high degree of polymer swelling. Macroporous resins consist of agglomerates of gel-type microspheres separated from each other by macroporesof 0.01-0.1µm. Unlike gel-type resins, these are prepared using compounds such as toluene or C$_4$-C$_{10}$ alcohols during polymerization. They do not polymerize and act as solvents for the monomers but not the polymer itself. Because of this, conduits are formed inside catalyst spheres leading to an artificial permanent porosity. It is worth noting that, while increased DVB% in gel-type resins is responsible for lower surface areas, in macroporous resins the opposite is true. Macroporous resins have far larger surface areas than gel-type ones. Despite this, a very high DVB% goes hand-in-hand with lower activities due the small number of active sites caused by having very few styrene monomers that can be sulfonated.

All polymers suffer from swelling when interacting with a solvent. Swelling of the resins in the solvent of use is crucial for their behavior as catalysts. The swelling capacity is understood as the variation in volume when interacting with liquid medium due to a difference in osmotic pressure between the inside and outside. Swelling takes place when dry resin comes into contact with polar substances producing an increase in surface area and porosity. Figure 5 represents the different behavior of gel-type and macroporous resins in regards to swelling.
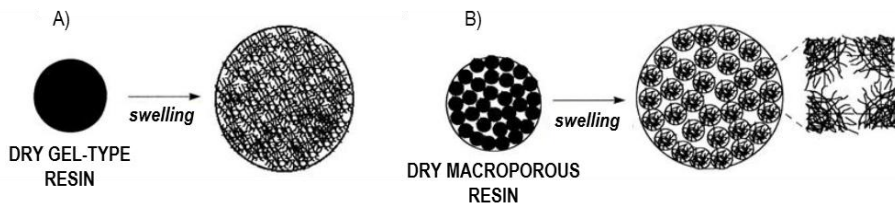
Figure 5. Morphological changes during swelling of a gel-type (A) and macroporous (B) catalyst particle.

Acid capacity is the number of accessible sulfonic groups in a completely swollen state and is determined by acid-base titration. It is usually expressed as mmoles per unit mass or volume. Resin density is the mass of dry resin per unit volume, and largely depends on matrix structure, the degree of cross-linking and number, nature and shape of functional groups. Ion-exchange resins have a limited amount of free and chemically bound water due to the hygroscopic properties of the functional groups they possess. Water content is defined as the quotient of water and total mass of hydrated resin.

Because ion-exchange resins must operate for long periods of time they must be chemically, thermally and mechanically stable. Mechanical stability is defined by resistance to compression and breaking. Macroporous resins are usually harder and more resistant because they possess a more cross-linked structure, but on occasion they might also be more brittle. Chemical stability is measured as the capacity for a resin to work in highly oxidizing conditions without experiencing changes in the polymeric matrix. Highly cross-linked resins are much more resistant to oxidizing conditions. Thermal stability allows a resin to withstand higher temperatures. This ability depends mostly on the structure of said resin. In sulfonic PS-DVB resins, thermal stability varies in relation depending on the degree of cross-linking (120-150ºC), and usually gel-type resins are more thermally stable (<150ºC). Given that thermal deactivation takes place by elimination of sulfonic groups, oversulfonated resins are slightly more stable that those that are conventionally sulfonated. A way to improve thermal stability consists in adding electron donating groups (like chlorine) to the sulfonated benzene ring, which rises the maximum operating temperature to 190ºC.

Because the structure and catalytic activity of a resin are intimately related, characterization of resin morphology is necessary to interpret resin effects observed in reactions in liquid media. Although the morphological data obtained from instrumental techniques such as N_2 absorption or Hg intrusion porosimetries are invaluable, they have the potentially severe limitation that they

refer to the dry state resin [55]. Using such data to interpret resin three--dimensional structures requires of the assumption that the morphology is not changed significantly when the resin is wetted with solvent. That is not true however; structures are severely affected by swelling both in macroporous and gel-type resins. Even in macroreticular resins which have permanent pores, new pores appear by the swelling of the polymer in suitable solvent. Therefore, in order to study the morphology of gel-type and macroreticular catalysts, other characterization techniques are needed.

Unfortunately there are no routine methodologies for evaluating the morphology of solvent-wet resins. Among the currently available methods, an appropriate procedure employed to reliably assess the morphology of ion-exchange resins in a swollen state has been the Inverse Steric Exclusion Chromatography (ISEC) technique [56]. ISEC is a chromatographic technique based on measurements of elution volumes of standard solutes with known molecular sizes, by using chromatographic column filled with the investigated swollen polymer [55]. Attempts to obtain porosimetric data from ISEC technique have been reported since 1975 [57]. In 1985 Jeřábek proposed an approach based on modelling of the porous structure as a set of discrete fractions, each composed of pores having simple geometry and uniform sizes. In this manner, gel-phase porosity is described as zones of different chain density [58]. In macroreticular structures a part of new open spaces in the range of mesopores can be characterized by a cylindrical pore model. However, this model is not applicable to describe spaces between polymer chains formed as a result of polymer swelling characteristic of gel-phase. The model developed by Ogston can more accurately describe the three-dimensional network of swollen polymer in which gel-phase micropores are described by spaces between randomly oriented rigid rods[59]. The characteristic parameter of this model is thespecific volume of the swollen polymer (volume of the free space plus that occupied by the skeleton), V_{sp}. The Ogston model also distinguishes between zones of swollen gel phase of different density or polymer chain concentration (total rod length per volume unit of swollen polymer, nm^{-2}). The morphology information given by ISEC technique has been used on successful correlation with catalytic activity of ion-exchangers in polar environments[60-63].In these works, it was observed that the accessibility of the reactants to acid centers was a key factor to describe the catalytic results.

4. OBJECTIVES

The current study is part of a larger study which goal it is to study catalysis by ion-exchange resins of PS-DVB in the synthesis of biomass-derived products. Given an absence of pre-existing data on the performance of these catalysts for the esterification of LA with BuOH, the goal of the present study is to ascertain whether or not sulfonated polystyrene-divinylbenzene acidic resins can be employed in the synthesis of BL from LA. Additionally, this study has been designed to:

1. Determine which types of ion-exchange acidic resins are more suitable for this reaction by comparing conversion and selectivity of different catalysts, and also which particular resin offers the most promise.

2. Deduce which resin properties hold the most influence on catalyst activity in the conditions the reaction is being carried out.

3. Compare resin performance with the data available in literature for other catalysts employed in this reaction.

5. EXPERIMENTAL SECTION

5.1. EXPERIMENTAL SET

Experiments for the synthesis of butyl levulinate were carried out using levulinic acid (ACROS ORGANICS, China, Code: 125140010) with purity of 98% and 2% water content. The other reagent used was 1-butanol (ACROS ORGANICS, Spain, Code: 232080025) with minimum purity 99.5% and water content under 0.5%.

PROPERTIES	1-BUTANOL	LEVULINIC ACID	BUTYL LEVULINATE [24-25]
CAS number	71-36-3	123-76-2	2052-15-5
Molecular mass (g/mol)	74.12	116.12	172.22
Density (kg/m^3)	810	1114.7	974
Melting point (ºC)	-90	33-35	Not available
Boiling point (ºC, at 760 mmHg)	118	245.5	237.8
Flash point (ºC)	35	137	92
Flammable Limits	11.3%(v) 1,4%(v)	Not available	Not Available
Hazard information	Flammable Corrosive Irritant/Toxic	Corrosive Irritant/Toxic	WHMIS: B3 Combustible liquid

Table 3. Compendium of reagent relevant properties.

In the chromatographic calibration the reagents used were 1-butanol and levulinic acid, as specified above. Additionally we also used butyl levulinate (SIGMA ALDRICH, Germany, Code: 101495705) with purity of 98% and 2% of acid levulinic content. Water (Milli-Q, Millipore) and dibutyl ether (DBE) (ACROS ORGANICS, Germany, Code: 149690010) with 99% purity and 1% of butanol content were also used for said calibration purposes.

Vapor pressure of the mixture's different components can also be found in literature [15]. Its dependence with temperature is defined by the parameters of the Antoine equation:

$$logP = A - \frac{B}{C + T}$$
(1)

where P is vapor pressure and T is temperature. The parameters A, B, and C can be found in Table 4. Vapor pressures of levulinic acid and butyl levulinate[15] are in kPa, while T is given in ºC. For 1-butanol, vapor pressure is given in mmHg and T also in ºC [64].

PARAMETER	1-BUTANOL	LEVULINIC ACID	BUTYL LEVULINATE
A	7.421	8.665	6.002
B	1351.555	3585.420	1603.570
C	179.810	293.474	164.907

Table 4. Parameters for the Antoine equation.

Pressurization of the reaction was performed with nitrogen gas of 99.9995% purity at 25atm overpressure. The chromatographic carrier gas was helium of 99.998% purity. Both were supplied by Abelló Linde (Barcelona, Spain).

Ion-exchange polystyrene-divinylbenzene (PS-DVB) sulfonated resins were used as catalysts. A wide range of commercial acidic resins was selected in order to screen for all different resin properties. The acidic resins used were Amberlyst 15 (A15), Amberlyst 16 (A16), Amberlyst 35 (A35), Amberlyst 36 (A36), Amberlyst 39 (A39), Amberlyst 46 (A46), Amberlyst 70 (A70) (Room & Haas); Purolite CT-224 (CT-224) (Purolite), and Dowex 50Wx8, Dowex 50Wx4, Dowex 50Wx2 (Dow Chemicals). Relevant resin properties are specified in Table 5.

The resins used in this study have two types of morphology: macroreticular (all Amberlyst) and gel-type (both Purolite and Dowex resins). The percentage of cross-linking agent (%DVB) relates to a greater or lesser stiffness of the polymeric structure of the resins. Their selection was meant to cover a great range of %DVB available in this type of ion-exchange resins.

There are three types of sulfonation present: conventionally sulfonated (CS), oversulfonated (OS) and surface-sulfonated (SS). The sulfonationtype influences acid capacity, and as a rule oversulfonated resins have a greater number of active sites, whereas surface sulfonated ones with sulfonic groups only in the outermost layer have very low acid capacity. On the other hand A70 is partially chlorinated and thus thermostable, with a maximum allowable temperature of 190ºC.

Catalyst	Type	Sulfonation type[a]	Acid capacity (mmol H+/g)[b]	%DVB	d_p[c] (mm)	Water retention (%)[c]	T_{max} (°C)[c]	d_{pore} (nm)[d]	ΣV_{pore} (cm³/g)[d]	ΣS_{pore} (m²/g)[d]	ΣV_{sp}[e] (cm³/g)
A15	macro	CS	4.81	20	0.74	52-57	120	12,4	0,616	192,00	0.622
A16	macro	CS	4.80	12	0.70	52-58	130	15,5	0,188	46,00	1.136
A35	macro	OS	5.32	20	0.51	51-57	150	12,6	0,720	199,00	0.504
A36	macro	OS	5.40	12	0.63	51-57	150	14,8	0,259	68,00	1.261
A39	macro	CS	4.82	8	0.71	60-66	130	15	0,155	56,00	1.643
A46	macro	SS	0.87	25	0.73	26-36	120	10,3	0,470	186,00	0.190
A70	macro	CS	2.55	8	0.57	53-59	190	13,2	0,220	66,00	1.149
CT-224	gel	OS	5.34	4	0.32	55	150	-	-	-	1.859
Dowex 50Wx2	gel	CS	4.83	2	0.499	74-82	150	-	-	-	2.677
Dowex 50Wx4	gel	CS	4.95	4	0.499	64-72	150	-	-	-	1.920
Dowex 50Wx8	gel	CS	4.83	8	0.499	50-58	150	-	-	-	1.404

(a) Conventionally sulfonated (CS), oversulfonated (OS) and surface sulfonated (SS).

(b) Titration against standard base.

(c) Manufacturer data.

(d) Swollen state (in water).

(e) Specific volume of swollen polymer in water, measured by ISEC technique.

Table 5. Properties of the acidic resin catalysts used in this study.

5.2. EXPERIMENTAL SETUP

The experimental set-up is detailed Fig. 6. The system consists of a 100ml stainless steel batch reactor (316 SS Autoclave Engineers) with a working overpressure of 25 atm. The reactor has a stirring, a relief valve, a pressure meter, a thermocouple, a baffle plate and a rupture disc.
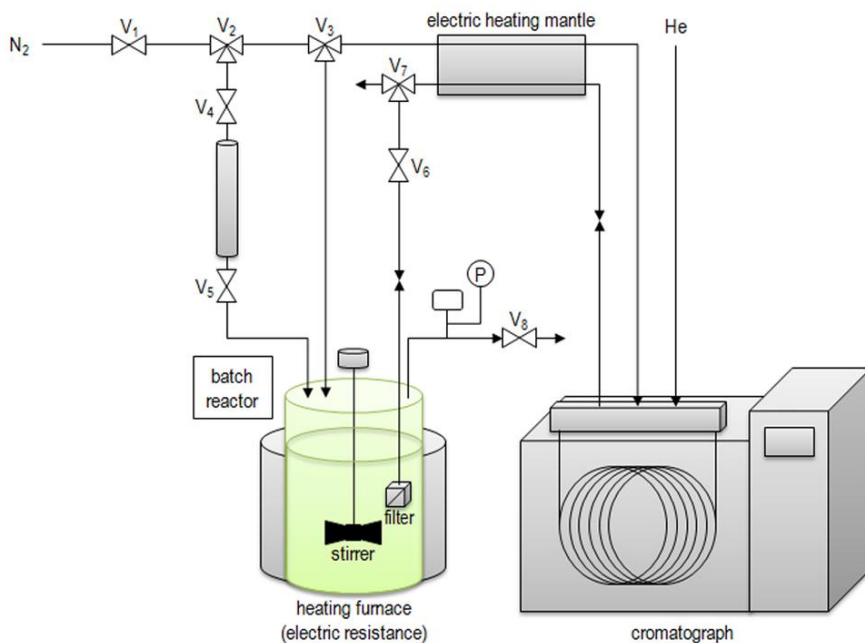
Figure 6.Scheme of the experimental set-up.

The stirring system consists of a turbine with four paddles of the axial up disperser mounted on a model Magnedrive II Series 0.7501 rotor. Stirring speed can be controlled through a frequency converter T-VERTER N2 SERIES. Alongside the turbine a stainless steel baffle plate 316 SS can be found whose function is to cut through the vortex created by stirring. A type K (cromel-alumel) termocouple measures the temperature inside the reactor. It is part of a proportional integral derivative (PID) temperature control system.

Pressure measurements are taken with a manometer (Labon Druckmessumformer CB6020) between the relief valve and the reactor. For the depressurization of the reactor the relief valve is used. It can be used in case of unforeseen pressure surges, but it is also used in order to

control flow in the sampling process. The rupture disc is prepared to resist up to a maximum pressure between 50.1 and 54.8 bars with 5% error margin. The heating system consists of an electric heating furnace TC-22 Pro 9 controlled by the reactor's internal temperature and that of its external wall surface both measured using thermocouples. Once reached the set-point temperature the system error margin is of ±0.1ºC.

The reactor has an entrance for N_2 gas and another from the catalyst injector. The catalyst injector is a stainless steel tube 316 SS in which the desired catalyst amount is deposited before a N_2 current pushes it inside the reactor by pneumatic transport.
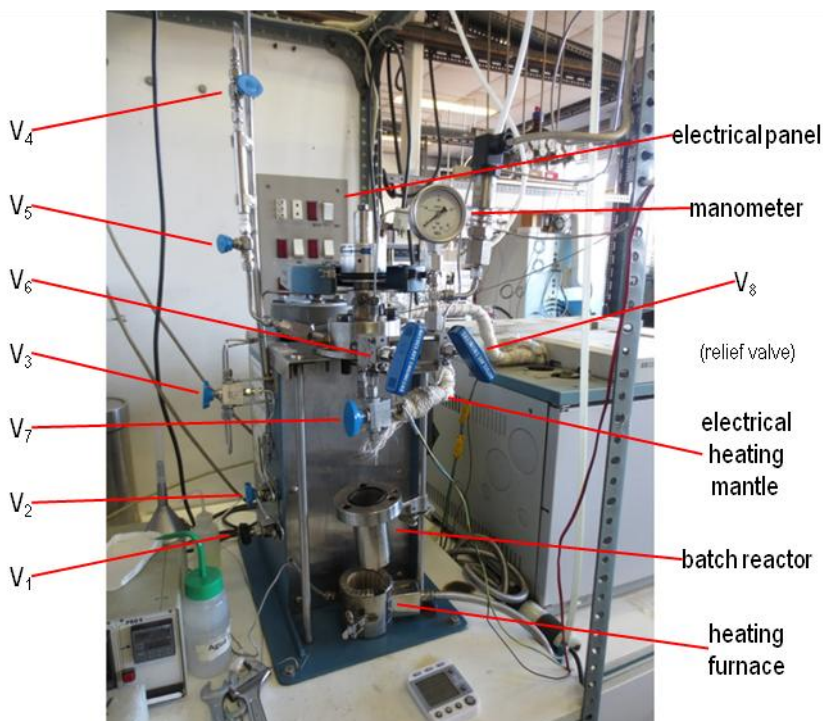
Fig 5.Disassembled experimental set-up.

Fig 6.A look into the internal accessories of the reactor.

Additionally sampling takes places through a sintered iron filter of 0.5 µm mesh size. System composition is as determined by means of in-line sampling to a gas chromatograph (Hewlett Packard HP 6890 GC Series, Germany, Serial # DE00020827) equipped with a thermal conductivity detector (TCD). The closed line connecting batch reactor to GC is kept at constant temperature 100ºC by an electric heating mantle. Sample aliquots (0.2µL) are carried by depression to the GC for analysis. Injection is carried out automatically by a mechanically actioned valve using synthetic air. The capillary column measurements are 20µm internal diameter, 0.5µm stationary phase thickness and 50m length (HP 190915-001, HP-Pona Methyl Siloxane). Stationary phase is methyl siloxane and the carrier gas used is He.

GC runs analysis method BULEVVAL.M. The sampling is based in injection through Valve 1 (6890 GC Valve) which takes 30s. Initially oven temperature is of 50ºC and it will rise 10ºC/min until it reaches 250ºC, andremains at 250ºC for 7min. Run time is of 27min, plus an additional 15min cool-down. System response are calibrated manually (Annex I).

5.3. EXPERIMENTAL PROCEDURE

5.3.1. Resin pre-treatment

Before being used, all acidic resins have been washed with water and dried at ambient temperature. Due to the wide distribution of particle diameter present in macroreticular resins, these have been sieved (at room temperature and humidity). The fraction selected was the one with smaller d_p present in all commercial samples (0.4 - 0.6 mm). Gel-type resins were used as

commercially available in the 50-100mesh size (0.149-0.297mm). Because PS-DVB resins are highly hygroscopic the following procedure was used to remove all water content. First, resins were dried for a minimum of 2h in an atmospheric oven at 110ºC, followed by drying in a vacuum oven at 110ºC and 10 mbar overnight. Water residual amount was about 1-3% depending on the resin (Fisher method).

5.3.2. Reactor loading

The feed mixture is prepared with the corresponding proportion of LA and BuOH. Reactants are weighed separately and introduced in the reactor. The volume of liquid inside the batch reactor must never surpass 70% (70mL) of its total volume because of safety concerns. The reactor is screwed shut with three retaining screws. Then valve V_1 is opened. Valve V_2 is turned to position 2, and valve V_3 into position 1, allowing N_2 to pass directly into the reactor bypassing the catalyst injector. The system is pressurized up to 25atm, and valve V_1 is closed. Following this the tightness of the system is verified if the manometer readings are stable. Valve V_1 is opened again for the duration of the experiment. The heating furnace is positioned around the reactor and fastened properly.

5.3.3. Experiment launching

After turning the switches of the electrical panel on, the stirring system (500rpm) is turned on alongside the computer terminal. The program *Microreactor Catalitic* by *LabView* is loaded into the computer. There the operating temperature inside the reactor (T_R) and that of the electric heating mantle in the sampling line (100ºC) are programmed. The surface temperature set point for the heating furnace is manually programmed40ºC above the operating temperature. Whilst the temperature inside the reactor reaches the set point, the program *Instrument Online* by *Chemstation* is loaded and BULEVVAL.M is selected as running method.

When operating temperature is stationary, the catalyst is injected. For this the topmost nut in the injection system (under valve V_4) is unscrewed, placing a funnel inside. The oven vacuum is broken, and the resin is weighed as quickly and accurately as possible. The dry resin is quantitatively funneled inside the injection cylinder, after which the topmost nut is screwed shut. Valve V_2 is turned to position 1, opening valves V_4 and V_5, forcing N_2 to pass through the catalyst injector. We induce a pressure drop in the reactor of 15atm by opening and closing the relief valve (V_5) repeatedly and rapidly (minimum of 5 times). We reverse position of valve V_2,

and close V_4 and V_5. At the same time the timer is started (t=0). The system is purged by opening and closing valve V_7 (switch to position 2).

5.3.4. Sampling

After the injection of catalyst the first sample is collected. Valve V_6 is opened whilst V_7 remains in position 1. After 6 min for the sample front to reach the GC, the analysis program is started by pressing the START button. The sample is returned to the reactor after 30s. Valve V_3 is switched to position 2, and opened and closed V_8 thrice (pressure drop of 10atm). Valve V_5 is closed and valve V_7 is switched to position 2 twice before being returned to position 1. Precautions must be taken for minute spraying may occur. Finally V_3 is returned to position 1, and the system is purged again (valve V_7). This process is repeated at 1h intervals throughout the experiment.

5.3.5. Clean-up

After the completion of the last GC sample analysis, the heating system is shut down from the control panel in the program *Microreactor Catalitic*. At the same time the stirring system is switched off. The corresponding switches in the electrical panel are turned off. The program Instrument Online is closed on the computer, and the GC is put on low-consumption mode. For this on the GC panel button OVEN the set point temperature is manually changed to 100ºC (then press ENTER). Next in the FRONT INLET button, press ON in the Gas Saver option. In the FRONT DET, press OFF in the Temp and Filament options. Close the valve V_1 and de-pressurize the reactor opening the relief valve V_8. Leave the system to cool down to ambient temperature.

After removing the three retaining screws, the reactor body is removed. Its contents is then weighted and filtered for the recovery of the catalyst. The reactor is washed with deionized water, ethanol and air dried with synthetic air. The filter is unscrewed from its support and placed in a beaker with hexane and left 20 min in an ultrasonic bath and later thoroughly dried with synthetic air. In order to clean the catalyst injector of an catalyst residue valve V_1 must be opened, V_2 turned to position 2 and open quickly valves V_4 and V_5. This is done repeatedly in order to create pressure surges that may dislodge any catalyst blockage present. The V_1, V_2, V_4 and V_5 are returned to their initial positions. The other reactor accessories are washed with deionized water and dried with synthetic air. The clean filter is screwed back on.

5.4. EXPERIMENTAL CONDITIONS

Experiments of 8h duration were carried out in the range of 80-120ºC and 26 atm in order to guarantee a reaction system in liquid phase. Operating temperature remains constant for the duration of the experiments. The screening of catalysts was done working with an excess of BuOH to avoid undesirable humin by-product formation. The molar ratio can be defined as:

$$R_{BuOH/LA} = \frac{n^o{}_{BuOH}}{n^o{}_{LA}} \left[\frac{mol}{mol}\right] \tag{2}$$

Preliminary experiments for different molar ratios were undertaken (R = 3, 5, 7, 9) and in the end the screening was done with $R_{BuOH/LA}$ = 3. The nominal capacity of the reactor is 100mL, but because of the presence of internal accessories and because of safety concerns the loading volume of reagents will be 70 ml, as previously mentioned.

$R_{BuOH/LA}$	m_{BuOH}	m_{LA}	V_{BuOH}	V_{LA}
3	41.12	21.81	50.77	19.23
5	46.20	14.70	57.04	12.96
7	48.78	11.09	60.22	9.78
9	50.34	8.90	62.15	7.85

Table 6. Reagent mass and volume for different molar ratios.

In order to screen for different catalysts it is decided to always use the same catalyst mass. The mass of dry catalyst used was 0.5g (0.8wt%) in all screening experiments. In preliminary experiments to determine operating temperature and molar ratio the catalyst mass used was of 1g (1.5wt%).

Stirring speed was fixed at 500 rpm. Evaluation of the possible effects of said variable on external mass transfer is not within the bounds of this study. Therefore, the assumption that resistance of external mass transfer does not affect reaction rates is assumed.

6. RESULTS AND DISCUSSION

6.1. REACTION MONITORING AND EVALUATION

Over the course of an experiment both the mole number of reagents and products are monitored. As can be observed in Figure 7, there is an exponential decrease in LA and an exponential increase of BL. As there are no major by-products, mol variation matches in both cases. Monitoring of butanol and water contents is more irregular, likely due to interactions with the polymeric catalyst structure and active sites. Figure 7 illustrates an essay with Amberlyst 39 (A39) as catalyst which is wholly representative of the rest.
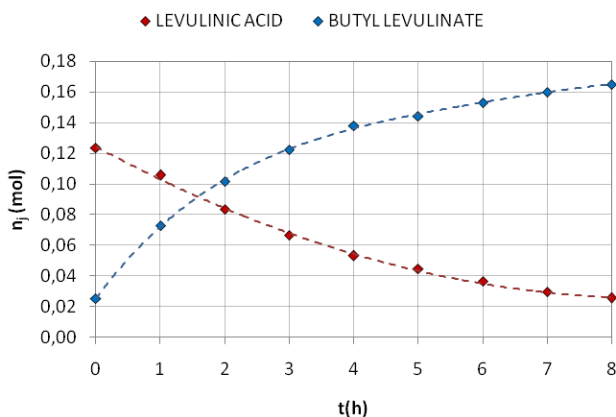
Figure 7. Moles of LA and BL over the course of the reaction time (catalyst A39, 0.75% catalyst mass).

For analysis and later comparison between different catalysts, the calculation of conversion (X_j) and selectivity (S^E_j) variables is necessary. Both are calculated based on the number of moles of each component. The reagent conversion in a discontinuous system is defined as:

$$X_j(t) = \frac{n°_j - n_j(t)}{n°_j} \left[\frac{mol}{mol}\right] \tag{3}$$

But because the consumed reagent produces other products with a known stoichiometry, conversion can be calculated from said products (Equations 4 and 5).

$$X_{LA} = \frac{n_{BL}}{n_{BL} + n_{LA}} \tag{4}$$

$$X_{BuOH} = \frac{n_{BL} + 2 \cdot n_{DBE}}{n_{BL} + n_{BuOH} + 2 \cdot n_{DBE}} \tag{5}$$

Selectivity of a reagent towards a product is defined as the quotient of the moles of product formed and the total moles of reagent consumed in a given reaction time. Considering the reaction stoichiometry selectivities can be written as:

$$S_{LA}^{BL} = \frac{n_{BL}}{n_{BL}} \tag{6}$$

$$S_{LA}^{H_2O} = \frac{n_{H_2O}}{n_{H_2O}} \tag{7}$$

$$S_{BuOH}^{BL} = \frac{n_{BL}}{n_{BL} + 2 \cdot n_{DBE}} \tag{8}$$

$$S_{BuOH}^{DBE} = \frac{n_{DBE}}{n_{BL} + 2 \cdot n_{DBE}} \tag{9}$$

$$S_{BuOH}^{H_2O} = \frac{n_{H_2O}}{n_{BL} + 2 \cdot n_{DBE}} \tag{10}$$

Throughout this study the reagent conversion referred to LA will be used because it is the limiting reagent. Additionally conversion has been calculated from reaction products (Equation 4) because GC chromatography analysis is more sensitive to concentration changes in BL than LA. On the other hand, selectivity will be referred to BuOH(Equations 8-10) because LA has no by-products and converts fully into BL and H_2O without any by-products.

6.2. SETTING THE EXPERIMENTAL CONDITIONS

In a screening study it is important to be able to compare the activity of different resins. In order to do that, the data obtained must show their differences to their best advantage. Adjusting the experimental conditions of the study must be undertaken first.

The experimental temperature and initial molar ratio conditions were adjusted with criteria of selectivity, and the catalyst mass according to the reaction rates observed. The recommended

experimental conditions given in literature for this reaction were taken as a starting point (Dharne et al.[50] and Maheria et al.[49]). Because of this, initial experimental conditions were set at 120ºC and a molar ratio 1:7 of LA to BuOH. An acidic polymer catalyst in the middle range of DVB% was chosen for an initial test run (A39, m_{cat} = 1.00g). Subsequent experiments were programmed at different temperatures (80, 100 and 120ºC) using fixed molar ratio, and later with different molar ratio (3, 5, 7 and 9) at fixed temperature in order to evaluate the influence of these parameters.

T (ºC)	X_{LA} (%)	S_{BuOH}^{BL} (%)
80	98.38	99.75
100	99.16	98.77
120	99.42	91.41

Table 7. Conversion and selectivity at 8h ($R_{BuOH/LA}$=7:1)
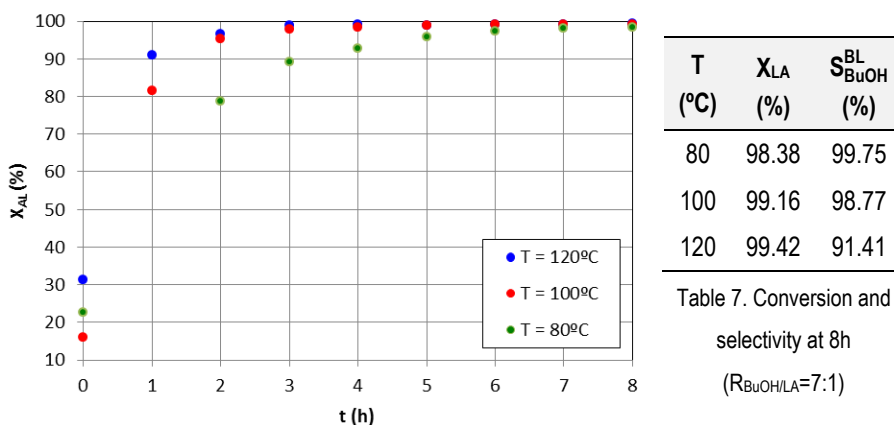
Figure 10. Conversion of LA over time at different operating temperatures ($R_{BuOH/LA}$=7:1).

Results at different temperatures showed that there was little difference given enough time(equilibrium conversion) (Figure 10). This was as expected considering that the reaction enthalpy (ΔH˚) of the esterification of LA with BuOH is only slightly endothermic at 7.14 ± 0,87 KJ·mol^{-1}[47]. Therefore temperature does not have a great influence on equilibrium conversion. Selectivity however, decreases more noticeably at higher temperatures (Table 7). The only relevant by-product that was detected is dibutyl ether (DBE). At 120ºC there was a 4,29% selectivity towards DBE. Although derived only from excess butanol, DBE formation hadto be evaluated, as another component in the LA esterification system. It will have to be removed by other physicochemical processes at a later point in any potential industrial process producing BL.

From an engineering perspective, higher temperature values achieve higher reaction rates and thus shorten reaction times. Short reaction times are conductive to a large number of cycles

in a batch process. Nonetheless high temperatures necessitate heating power, which is more expensive in both money and resources. As potential selectivity problems are more readily apparent at higher temperature, the evaluation of the effects of molar ratio was undertaken at 120ºC (the maximum work temperature all catalysts can withstand).
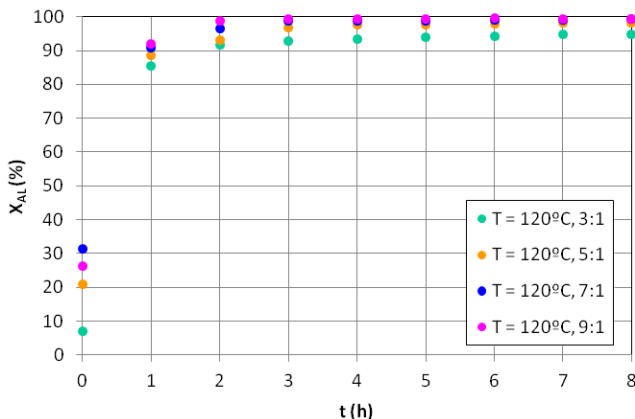
$R_{BuOH/LA}$	X_{LA} (%)	S_{BuOH}^{BL} (%)
3	95.05	98.57
5	98.29	95.35
7	99.15	91.41
9	99.60	88.80

Table 8. Conversion and selectivity at 8h (120ºC)

Figure 11.Conversion of LA over time at different initial molar ratios BuOH/LA.

Classically the esterification of LA has always been carried out with alcohol excess. The need to avoid high concentrations of LA in order to prevent polymerization and the formation of humins is often cited. Probably this can only be applicable when unrefined LA crudes are used as reagents, which often contain remnants of the glucose hydrolysis. When working with purified LA it was found that selectivity does in fact improve at lower molar ratios (Table 8).No other by-product was detected by GC and no solid precipitates were observed. Conversion and reaction rates decreased for lower molar ratios, nonetheless it is not as marked a tendency as the aforementioned improvement to selectivity. Furthermore, closer molar ratios to 1 are always desirable from an economic perspective, with less expenditure of butanol and greater BL production in each batch.

Present experiments strived to determine if it would be possible to employ lower molar ratios than those traditionally used in literature[49-50]. However, at molar ratios under 3:1it was found that miscibility problems arose. At these lower molar ratios of BuOH to LA, the formation of two liquid phases due to the formation of water during the course of the reaction was unavoidable, which is an undesirable prospect for several reasons. Firstly, the formation of aggregates affects

conversion severely. The presence of two separate liquid phases marks a significant departure from an ideal reactor (microfluidic). Secondly, the capacity to determine system composition at different points in time would be greatly affected. With the analysis system presently at our disposal it is not possible to correctly analyze samples from a biphasic system. The problem can be summarized in a failure to correctly calibrate the GC and the difficulty of taking samples representative of the contents of the reactor. Correct analysis should require a titration analysis and with the present experimental set-up this would require determining only final composition.

Because of all of the above it was resolved that any further experiments would take place at a molar ratio of 3:1. Working at high temperature was discarded because no further selectivity problems were detected working at 120ºC that could be used to judge catalyst performance. DBE is only formed in small amounts from the cheaper excess reagent below that temperature. Thus, it was considered more interesting to determine the potential of acidic ion-exchange catalysts to work at lower temperatures and further experiments took place at 80ºC.
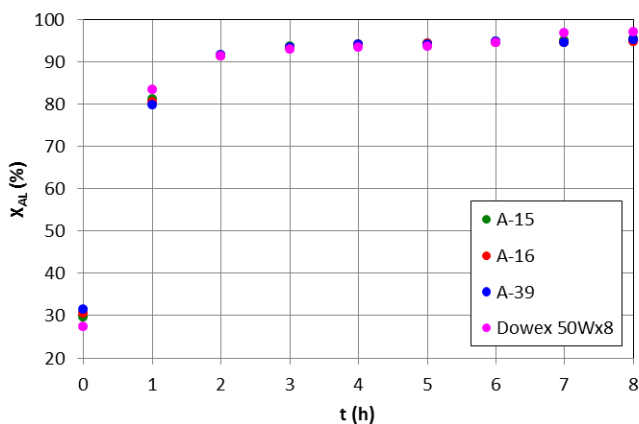
Figure 12. Conversion of LA over time for different acidic ion-exchange resins (1,5% catalyst mass, 80ºC).

The catalyst mass used was settled at a lower value than that used for determining experimental conditions. Experiments with different catalysts and catalyst mass of 1.00g (1.5wt%) showed almost identical behaviour and all approached equilibrium in under 3h (Figure 6). Experiments with lower catalyst mass percentage showed noticeable differences in performance between catalysts. In the screening experiments catalyst mass was lowered to 0.5g (0.75wt%).

6.3. A SCREENING STUDY OVER ION-EXCHANGE RESINS

The conducted experiments confirm that acidic polymeric catalysts can be used in order to obtain very high conversion and selectivity in the esterification of LA with BuOH to BL at low temperature (Figure 13).

Through a blank it was found that at 80ºC without catalyst, the reaction achieved a conversion of 24% after 8h. This indicates that reaction takes place homogeneously without catalyst, although with rather low conversion. The short pre-heating process previous to catalyst injection produces a small amount of BL and water. Conversions usually fall between 10-25%.

As mentioned, the most relevant by-product is dibutyl ether (DBE), even though it is never more than 2% in mass. At operating temperature of 80ºC and 0.75% catalyst mass at higher temperature, selectivity towards BL remains over 99% (Table 9).Selectivity will not be further commented upon because it adds nothing relevant to the screening study. It only underscores that acidic PS-DVB polymeric resins are eminently suited to catalyze this esterification reaction in a clean low-temperature process.

Catalyst	X_{AL} (2h)	X_{AL} (4h)	X_{AL} (8h)	S_{BuOH}^{BL} (8h)
Amberlyst 15	39.26	52.73	69.82	99.66
Amberlyst 16	41.24	55.68	74.89	99.62
Amberlyst 35	40.52	55.04	70.93	99.82
Amberlyst 36	46.66	59.67	78.14	99.53
Amberlyst 39	54.94	72.20	86.61	99.86
Amberlyst 46	---	45.70	63.95	99.63
Amberlyst 70	46.80	62.79	81.03	99.85
CT-224	60.95	77.39	90.60	99.86
Dowex 50Xx2	71.83	86.30	93.59	99.87
Dowex 50Xx4	66.83	82.46	92.35	99.87
Dowex 50Xx8	48.19	63.34	81.26	99.70

Table 9. Conversion values at 2, 4 and 8h reaction time and the final selectivity values.

The catalyst with highest activity was Dowex 50Wx2 (Figure 13). Overall gel-type resins presented better LA conversions than macroporous ones (not yet in equilibrium). Acidic ion-exchange resins swell to a higher degree when submerged in polar solvent medium. Because of the high polarity of LA and the formation of water, swelling is favored in the reaction medium. At

the same time gel-type resins have a higher swelling capacity than macroporous ones because of lower concentrations of cross-linking agent (DVB) which confers them less rigid structures. It appears also that catalysts with greater capacity for swelling favor LA esterification conversions. Thus resins with a lesser degree of cross-linking (DVB%) present higher reaction rates.
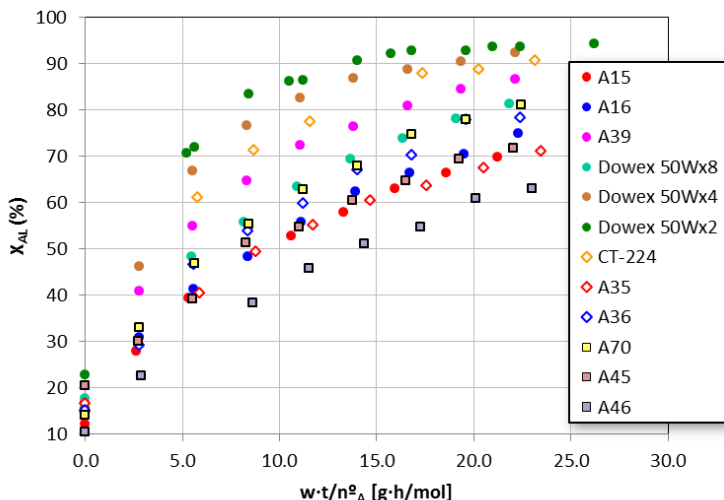
Figure 13.Comparison of conversion evolution of LA over timefor various catalysts.

Incidentally, CT-224 was less active than Dowex 50Wx4 (both 4% DVB) despite having a higher number of active sites. This fact might be because resin oversulfonation confers a certain additional stiffness to the polymeric structures, which impedes swelling. This was not always the case with other oversulfonated resins and their conventionally sulfonated counterparts. One could speculate that acid capacity does not have any effect on reaction rates. A15 and A35 have 20% DVB (high degree of cross-linking) and no differences between them were observed in their catalytic performance. On the other hand, A36 was marginally better than A16 (12% DVB). In this case where high amounts of cross-linking agent furnish a very rigid structure, a higher number of active sites (surface macropores) can slightly counteract this effect.

The lowest activity was that of A46, which is surface-sulfonated and therefore has a very low number of active sites. LA conversion was not much lower than those obtained with A15, A16 and A35 (9% lower conversion). This suggests that for resins with a high degree of cross-linking (DVB>12%), swelling might be so poor that the reaction takes place mainly on active

sites close to the surface. This supports the hypothesis that a good swelling capacity in BuOH is desirable for a catalyst of the LA esterification reaction.

Although A70 also has a lower number of active sites, reaction rates are on par with Dowex 50Wx8, yet lower than A39 (all 8% DVB). Presumably the inner structure of the active sites of A70, due to the electron donating chloride groups often present in thermostable resins confers a higher acid force to said sites, which might have a compensatory effect.

The Dowex 50Wx2 experiment was replicated twice (with differing catalyst mass) with perfect overlap in the tendency of conversion vs. normalized time. Therefore it has been concluded that the experiments of this screening study are fully replicable and experimental error is less than 3-5%.

This study has attempted to ascertain which catalyst properties have a greater effect on catalyst efficiency for the specific reaction of the esterification of LA with BuOH. To this effect the different relevant properties of PS-DVB acidic resins have been related to conversion at different reaction times (Figure 14).

It was found that although the acid protons are those which allows the catalytic process in the first place, acid force is of secondary importance in the choice of catalyst for this reaction. As can be observed, there is no clear marked correlation between the number of active sites (acid capacity) and conversion. Many resins with similar acid capacity show very different conversion. This suggests that other structural parameters are of greater importance in resin catalyst efficiency.

Permanent pore (macropore) measurements in diameter, global surface and volume are only relevant to macroporous resins. Nonetheless these parameters can give us a clue in regards to issues of accessibility. It appears that larger macropores have slightly larger conversions overall. This tendency is not as marked as could be expected in the case of accessibility issues because macropores have an average diameter ten times larger than estimated molecule length (d_{AL}=6.78Å, d_{BL}=14.29Å). A larger global macropore surface and volume can generally be related to lower conversions. This can easily be explained because larger pore surfaces and volumes correspond with highly cross-linked and stiff resins.
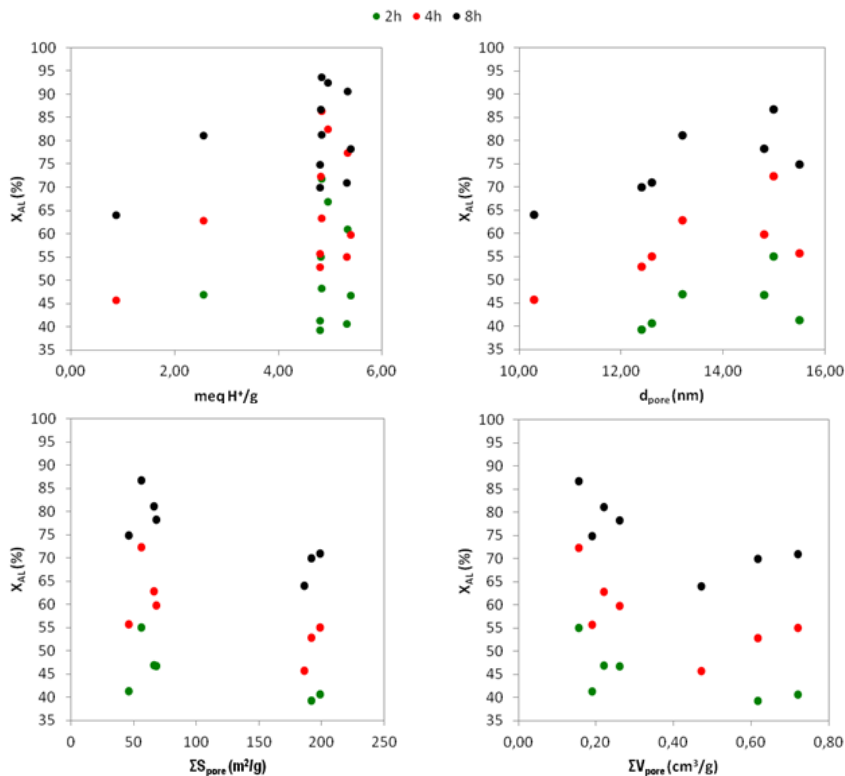
Figure 14. Conversion achieved at 2, 4 and 8h reaction time versus acid capacity, macropore diameter (d_{pore}), global macropore surface (ΣS_{pore}) and global macropore volume (ΣV_{pore}).

More important to catalyst efficiency than catalyst pore size is molecule access to said pores, which is facilitated by the polymer swollen state. Polar molecules show an affinity for sulfonic groups and their network of hydrogen bonds. When immersed in a polar solvent polymeric catalysts swell because of the interaction of the medium with the catalyst structure. In the swollen state appear a number of mesopores (2-50nm) and micropores (d<2nm), creating a larger number of accessible active sites on top of the macropore (d>50nm) surface sites. The amount of cross-linking agent (%DVB) used in catalyst synthesis determines the formation of macropores (permanent pore structure), but even in the macroreticular resins new pores appear by the swelling of the polymer in suitable solvent. A more solid permanent structure with greater cross-linking hinders polymer swelling by locking polymer chains together and limiting their ability to uncoil, rendering them less flexible. As can be seen in Figure 15, conversion of LA

decreases with higher %DVB in almost linear fashion. At the same given value of %DVB several data points with slightly different conversions appear which are due to differences in acid capacity.
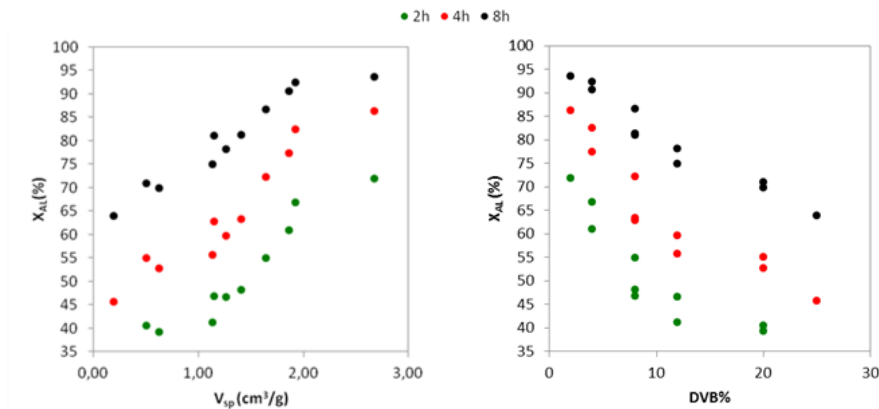
Figure 15. Conversion achieved at 2, 4 and 8h reaction time versus specific volume of swollen polymer in water (measured by ISEC technique) and %DVB.

Globally, higher reaction rates roughly correspond with large V_{sp} values (Figure 15). This tendency is well-defined and consistent with all of the above. V_{sp} gives an accurate idea of the magnitude of polymer swelling in polar medium. Nonetheless, the matter is more complex. The polymeric structure does not swell uniformly when immersed in any solvent. When modeling the porous structure, it can be described as a set of discrete fractions in which gel-phase porosity is described as zones of different chain density. Different resins contain uneven ratios of the different fractions defined. It can be seen in Figure 16, that the preponderance of one fraction or another has as much impact on catalyst activity as the total amount of V_{sp}. In almost all cases of high activity rates, large medium to low chain density fractions were reported (0.1-0.4nm/nm^3). Thus more densely packed polymeric structures in the swollen state are found to be disadvantageous to higher reaction rates.

Figure 16 can also shed light as to why it has been found during this screening that A39 (macroporous) and Dowex 50Wx8 (gel-type) have noticeably different activity rates despite having equal %DVB, acid capacity and being both conventionally sulfonated. This seems to contradict the general tendency for gel-type resins to have overall higher conversion. It can be seen that Dowex 50Wx8 has not only lower V_{sp}, but contains mostly densely packed polymer

chains. It can also confirm our speculations about the nature of the disadvantage of CT-224 in regarding Dowex 50Wx4. CT-224 does have denser structure as well as a lower V_{sp}. It can also be observed that A70 structures in the swollen state fall entirely in the aforementioned range of low chain density fractions in which higher conversions are reported. Thus the fact that conversion in A70 is reported to be relatively high regardless of its lower acid force can be chalked up not only to the inner structure of its active sites but to the resulting lighter density of the entire resultant structure.
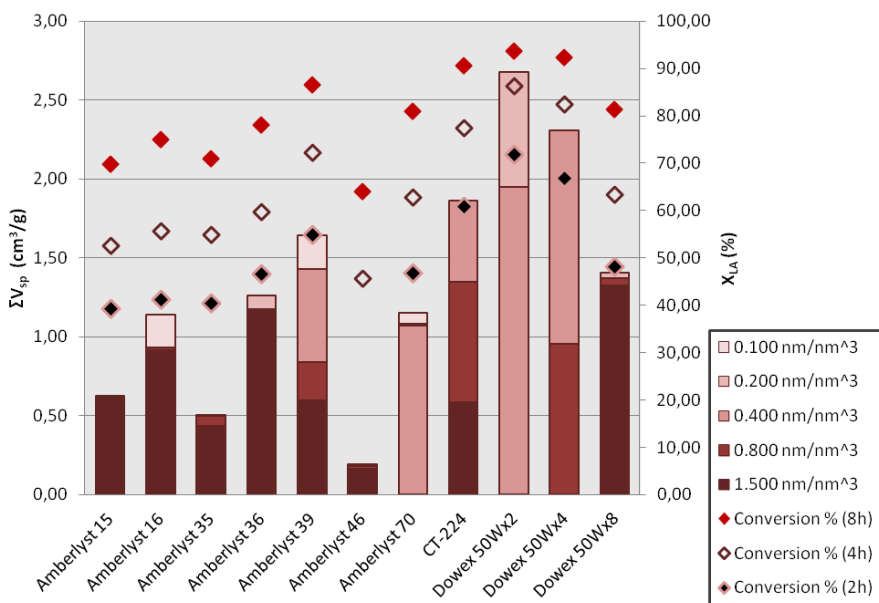
Figure 16. Conversion achieved at 2, 4 and 8h reaction time Vsp of various density fractions of a catalyst.

To summarize, it can be ruled that the best perspective catalysts for the esterification of LA with BuOH is Dowex 50Wx2, or failing that, either Dowex 50Wx4, CT-224 or A39. All of these have high selectivity and high catalytic activity (conversion of LA over 85%). This results point out that this acidic ion-exchange catalysts are competitive versus other heterogeneous catalysts with which this reaction has been studied previously in literature (See section 3.2.).

7. CONCLUSIONS

This study has proven that the esterification of levulinic acid with butanol can take place at low temperature with high reaction rates if the appropriate acidic ion exchange resins are employed. This reaction has high selectivity (over 98%) when starting from pure reagents.

Gel-type resins with higher swelling show better activity as a whole. Of the catalysts sampled and in the conditions this study was carried out, Dowex 50Wx2 was found to be the most active.

Resin swelling capacity is the catalyst property that has the most control over catalyst efficiency. The reaction rates increase significantly when the swollen polymer phase is highest and there are large parts with low-medium polymer density. Reaction rates improve as the degree of polymer cross-linking diminishes (%DVB). On the other hand resin acid capacity does not have as immediate an effect on catalyst activity.

Ion-exchange catalysts have been found to be more efficient than zeolites quoted in literature[49], because they have been proven to have better yields at lower temperatures and higher concentrations of LA without humins. Compared with heteropolyacid supported on acid-treated clay montmorillonite[50], which have similar activity rates and selectivity (in literature), ion-exchange resins are cheaper and readily commercially available and thus more readily applicable to existent and new industrial processes.

Nonetheless, further testing could be applied to acidic ion exchange resins in order to ascertain whether or not they are eminently suitable to catalyze this reaction in an industrial setting. Follow-up studies of the lifespan and reusability of these catalysts would be necessary, as well as further studies with industrial LA crudes.

8. REFERENCES

1. Regalbuto, J. R. Cellulosic biofuels - got gasoline? *Science.* **2009**, *325*, 822-824.
2. Climent, M. J.; Corma, A.; Iborra, S. Conversion of biomass platform molecules into fuel additives and liquid hydrocarbon fuels. *Green Chem.* **2014**, *16(2)*, 516-547.
3. Demirbas, A. Competitive liquid biofuels from biomass.*Appl. Energy.* **2011**, *88(1)*, 17-28.
4. Hayes, D. J. Second-generation biofuels: Why they are taking so long. *Wiley Interdiscip. Rev. Energy Environ.* **2013**, *2(3)*, 304-334.
5. Banerjee, S.; Mudliar, S.; Sen, R.; Giri, B.; Satpute, D.; Chakrabarti, T.; Pandey, R. Commercializing lignocellulosic bioethanol: technology bottlenecks and possible remedies.**2009**, *4(1)*, 77-93.
6. Virent Energy Systems Inc., (**2010**). Virent and Shell Start World's First Biogasoline Production Plant. [Press Release] Retrieved fromhttp://www.virent.com/news/virent-and-shell-start-world%E2%80%99s-first-biogasoline-production-plant/ [Accessed 22 May 2015].
7. Envergent Technologies, (**2010**). The production of electricity from wood and other solid biomass.RTP/Advanced cycle vs. combustion steam cycles or why not simply combust? [White Paper] Retrieved from http://www.ensyn.com/about-ensyn/about-ensyn-product/ [Accessed 22 May 2015].
8. Jonietz, E. Oil from Wood. Startup Kior has developed a process for creating "biocrude" directly from biomass.*MIT Technol. Rev*. **2007** [online] Available at http://www.ensyn.com/about-ensyn/about-ensyn-product/ [Accessed 22 May 2015].
9. Corma, A.; Iborra, S.; Velty, A. Chemical routes for the transformation of biomass into chemicals.**2007**, *107(6)*, 2411-2502.
10. Ghorpade, V.; Milford, H. Industrial applications for Levulinic Acid. In Campbell, G. M.; Webb,C.; McKee, S. L. (Eds.)*Cereals: Novel Uses and Processes* (Springer US, Boston, MA, **1997**), p. 49-56.
11. Hayes, D. J.; Fitzpatrick, S.; Hayes, M. H. B.; Ross, J.R.H. The Biofine Process - Production of Levulinic Acid, Furfural, and Formic Acid from Lignocellulosic Feedstocks. In Kamm, B.; Gruber, P. R.; Kamm, M. (Eds.) *Processes and Products: Status Quo and Future Directions* (Wiley-VCH, Weinheim, Germany, **2006**).
12. Bozell, J. J.; Moens, L.; Elliott, D. C.; Wang, Y.; Neuenscwander, G. G.; Fitzpatrick, S. W.; Bilski, R. J.; Jarnefeld, J. L. Production of levulinic acid and use as a platform chemical for derived products. **2000**, *28(3-4)*, 227-239.
13. E4tech, RE-CORD, WUR (**2015**). From the Sugar Platform to biofuels and biochemicals. Final Report of the European Commission Directorate-General Energy. Retrieved from https://ec.europa.eu/energy/sites/ener/files/documents/EC%20Sugar%20Platform%20final%20report.pdf [Accessed 22 May 2015].
14. Grand View Research (**2014**). Levulinic Acid Market Analysis And Segment Forecasts To 2020. Retrieved from http://www.grandviewresearch.com/industry-analysis/levulinic-acid-market.
15. Lomba, L.; Giner, B.; Bandrés, I.; Lafuente, C.; Pino, M. R.; Physicochemical properties of green solvents derived from biomass. *Green Chem.* **2011**, *13(8)*, 2062-2070.
16. Heineman, H. H.; Howard, C. L.; Rogers, H. J. Combustion resistant rubber latex foam containing a hydrocarbon mineral oil and a reinforcing styrene polymer. U.S. Patent 3,107,224, Oct. 15, **1963**.
17. Bader, A. R. Addition products of phenols and keto acids and derivatives of the same. U.S. Patent 2,933,520, Apr. 19, **1960**.
18. Govers, F. X. Solvent refining oil. U.S. Patent 2,087,473, July 20, **1937**.
19. Yontz, D. J.; Fragrant formulations, methods of manufacture thereof and articles comprising the same. U.S. Patent Application 2011/0274643 A1, Nov. 10, **2011**.

20. Bloom, P. D. Levulinic acid ester derivatives as reactive plasticizers and coalescent solvents. U.S. Patent Application 2010/0216915 A1, Aug. 26, **2010**.

21. Rieth, L.R.; Leibig, C. M.; Pratt, J. D.; Jackson, M. Latex coating compositions including carboxy ester ketal coalescents, methods of manufacture, and uses therof. U.S. Patent Application 2012/0041110 A1, Feb. 16, **2012**.

22. Démolis, A.; Essayem, N.; Rataboul, F. Synthesis and applications of alkyl levulinates. *ACS Sustain. Chem. Eng.***2014**, *2(6)*, 1338-1352.

23. Sah, P. P. T.; Ma, S. Levulinic acid and its esters. *J. Am. Chem. Soc.* **1930**, *52(12)*, 4880-4883.

24. Schuette, H. A.; Cowley, M. A. Levulinic acid II. The vapour pressures of its alkyl esters C_6-C_{10}.*J. Am. Chem. Soc.* **1931**, *53(9)*, 3485-3489..

25. Cox, G. J.; Dodds, M. L. Some Alkyl Esters of Levulinic Acid. *J. Am. Chem. Soc.* **1933**, *55(8)*, 3391-3394.

26. Pasquale, G.; Vázquez, P.; Romanelli, G.; Baronetti, G. Catalytic upgrading of levulinic acid to ethyl levulinate using reusable silica-included Wells-Dawson heteropolyacid as catalyst. *Catal. Commun.* **2012**, *18*, 115-120.

27. Fernandes, D. R.; Rocha, A. S.; Mai, E. F.; Mota, C. J. A.; Teixeira Da Silva, V. Levulinic acid esterification with ethanol to ethyl levulinate production over solid acid catalysts. *Appl. Catal. A Gen.* **2012**, *425-426*, 199-204.

28. Nandiwale, K. Y.; Sonar, S. K.; Niphadkar, P. S.; Joshi, P. N.; Deshpande, S. S.; Patil, V. S.; Bokade, V.V.; Catalytic upgrading of renewable levulinic acid to ethyl levulinate biodiesel using dodecatungsto-phosphoric acid supported on desilicated H-ZSM-5 as catalyst. *Appl. Catal. A Gen.***2013**, *460-461*, 90-98.

29. Yan, K.; Wu, G.; Wen, J.; Chen, A. One-step synthesis of mesoporous $H_4SiW_{12}O_{40}$-SiO_2 catalysts for the production of methyl and ethyl levulinate biodiesel. *Catal. Commun.* **2013**, *34*, 58-63.

30. Patil, C. R.; Niphadkar, P. S.; Bokade, V. V.; Joshi, P. N. Esterification of levulinic acid to ethyl levulinate over bimodal micro-mesoporous H/BEA zeolite derivatives. *Catal. Commun.* **2014**, *43*, 188-191.

31. Su, F.; Ma, L.; Song, D.; Zhang, X.; Guo, Y. Design of a highly ordered mesoporous $H_3PW_{12}O_{40}$/ZrO_2–Si(Ph)Si hybrid catalyst for methyl levulinate synthesis. *Green Chem.* **2013**, *15(4)*, 885-890.

32. Yadav, G. D.; Yadav, A. R.; Synthesis of ethyl levulinate as fuel additives using heterogeneous solid superacidic catalysts: Efficacy and kinetic modeling. *Chem. Eng. J.* **2014**, *243*, 556-563.

33. Su, F.; Wu, Q.; Song, D.; Zhang, X.; Wang, M.; Guo, Y. Pore morphology-controlled preparation of ZrO_2-based hybrid catalysts functionalized by both organosilica moieties and Keggin-type heteropoly acid for the synthesis of levulinate esters. *J. Mater. Chem. A* **2013**, *1(42)*, 13209-13221.

34. Oliveira, B. L.; Teixeira Da Silva, V. Sulfonated carbon nanotubes as catalysts for the conversion of levulinic acid into ethyl levulinate. *Catal. Today.* **2014**, *234*, 257-263.

35. Budarin, V. L.; Clark, J. H.; Luque, R.; Macquarrie, D. J.; Versatile mesoporous carbonaceous materials for acid catalysis. *Chem. Commun. (Camb).***2007**, *(6)*, 634-636.

36. Melero, J. A.; Morales, G.; Iglesias, J.; Paniagua, M.; Hernández, B.; Penedo, S. Efficient conversion of levulinic acid into alkyl levulinates catalyzed by sulfonic mesostructured silicas. *Appl. Catal. A Gen.* **2013**, *466*, 116-122.

37. Kuwahara, Y.; Kaburagi, W.; Nemoto, K.; Fujitani, T. Esterification of levulinic acid with ethanol over sulfated Si-doped $ZrO2$ solid acid catalyst: Study of the structure-activity relationships. *Appl. Catal. A Gen.* **2014**, *476*, 186-196.

38. Lee, A.; Chaibakhsh, N.; Rahman, M. B. A.; Basri, M.; Tejo, B. A. Optimized enzymatic synthesis of levulinate ester in solvent-free system. *Ind. Crops Prod.* **2010**, *32(3)*, 246-251.

39. Chang, C.; Xu, G.; Jiang, X. Production of ethyl levulinate by direct conversion of wheat straw in ethanol media. *Bioresour. Technol.* **2012**, *121*, 93-99.

40. Fagan, P. J.; Korovessi, E. Ernest, L.; Mehta, R. H.; Thomas, S. M. Preparation of Levulinic Acid Esters and Formic Acid Esters from Biomass and Olefins; Compositions Prepared Thereby; and Uses of the Compositions as Fuels Additive. U.S. Patent Application 2003/0233011 A1, Dec. 18, **2003**.

41. Liu, R.; Chen, J.; Huang, X.; Chen, L.; Ma, L.; Li, X. Conversion of fructose into 5-hydroxymethyl-furfural and alkyl levulinates catalyzed by sulfonic acid-functionalized carbon materials. *Green Chem*. **2013**, *15(10)*, 2895-2903.

42. Peng, L.; Lin, L.; Zhang, J.; Shi, J.; Liu, S. Solid acid catalyzed glucose conversion to ethyl levulinate. *Appl. Catal. A Gen.* **2011**, *397(1-2)*, 259-265.

43. UFA Limited. Diesel fuel characteristics and resources. **2009** [online] Available at http://www.ufa.com/petroleum/resources/fuel/diesel_fuel_resources.html [Accessed 22 May 2015].

44. Christensen, E.; Yanowitz, J.; Ratcliff, M.; McCormick, R. L.; Renewable oxygenate blending effects on gasoline properties. *Energy and Fuels.* **2011**, *25(10)*, 4723-4733.

45. Joshi, H.; Moser, B. R.; Toler, J.; Smith, W. F.; Walker, T. Ethyl levulinate: A potential bio-based diluent for biodiesel which improves cold flow properties. *Biomass and Bioenergy.***2011**, *35(7)*, 3262-3266.

46. Christensen, E.; Williams, A.; Paul, S.; Burton, S.; McCormick, R. L. Properties and performance of levulinate esters as diesel blend components. *Energy and Fuels*. **2011**, *25(11)*, 5422-5428.

47. Bart, H. J.; Reidetschmger, J.; Schatka, K.; Lehmann, A. Kinetics of Esterification of Levulinic Acid with n-Butanol by Homogeneous Catalysis. *Ind. Eng. Chem. Res.* **1994**, *33(1)*, 21-25.

48. Hishikawa, Y.; Yamaguchi, M.; Kubo, S.; Yamada, T. Direct preparation of butyl levulinate by a single solvolysis process of cellulose. *J. Wood Sci.* **2013**, *59(2)*, 179-182.

49. Maheria, K. C.; Kozinsji, J.; Dalai, A.; Esterification of levulinic acid to n-butyl levulinate over various acidic zeolites. *Catal.Letters.* **2013**, *143(11)*, 1220-1225.

50. Dharme, S.; Bokade, V. V.; Esterification of levulinic acid to n-butyl levulinate over heteropolyacid supported on acid-treated clay. *J. Nat. Gas Chem.* **2011**, *20(1)*, 18-24.

51. Yadav, G. D.; Borkar, I. V. Kinetic modeling of immobilized lipase catalysis in synthesis of n -butyl levulinate. *Ind. Eng. Chem. Res*. **2008**, *47(10)*, 3358-3363.

52. Izquierdo, J. F.; Cunill, F.; Tejero, J.; Iborra, M.; Fité, C. Cinética de las reacciones químicas (EdicionsUniversitat Barcelona., 1st Ed., Barcelona, **2004**, p. 143-267.

53. Leofanti, G.; Surface area and pore structure of catalyst. *Catal.Today.***1998**, *41*, 207-219.

54. Barbaro, P.; Liguori, F.; Ion Exchange Resins: Catalyst Recovery and Recycle. *Chem. Rev.* **2009**, *109(2)*, 515-529.

55. Buchmeiser, M. R. Polymeric Materials in Organic Synthesis and Catalysis (Wiley-VCH, Weinheim, Germany, **2006**) p. 29-30.

56. Jeřábek, K. Inverse Steric Exclusion Chromatography as a Tool for Morphology Characterization. In Potschka, M.; Dubin, P. L. (Eds.) *ACS Symposium Series:Strategies in size exclusion chromatography* (American Chemical Society, USA, 1996) p. 221-224.

57. Halász, I.; Martin, K. Bestimmung der Porenverteilung (10 – 4000 Å) von Festkörpern mit der Methode der Ausschluß-Chromatographie. *Berichte der Bunsengesellschaft für Phys. Chemie.* **1975**, *79(9)*, 731-732.

58. Jeřábek, K.Characterization of Swollen Polymer Gels Using Size Exclusion Chromatography. *Anal. Chem*. **1985**, *57*, 1598-1602.

59. Ogston, A. G.; The spaces in a uniform random suspension of fibres. *Trans. Faraday Soc*. **1958**, *54*, 1754-1757.

60. Buttersack, C. Accesibility and Catalytic Activity of Sulphonic Acid Ion-Exchange Resins in Different *Solvents. React. Polym.* **1989**, *10(2)*, 143-164.

61. Tejero, J.; Cunill, F.; Iborra, M.; Izquierdo, J. F.; Fité, C. Dehydration of 1-pentanol to di-n-pentyl ether over ion-exchange resin catalysts. *J. Mol. Catal. A Chem*. **2002**, *182-183*, 541-554.

62. Bringué, R.; Iborra, M.; Tejero, J.; Izquierdo, J. F.; Cunill, F.; Fité, C.; Cruz, V. J. Thermally stable ion-exchange resins as catalysts for the liquid-phase dehydration of 1-pentanol to di-n-pentyl ether (DNPE). *J. Catal.* **2006**, *224(1)*, 33-42.

63. Guilera, J.; Bringué, R.; Ramírez, E.; Iborra, M.; Tejero, J. Synthesis of ethyl octyl ether from diethyl carbonate and 1-octanol over solid catalysts. A screening study. *Appl. Catal. A Gen*. **2012**, *413-414*, 21-29.

63. Kemme, H. R.; Kreps, S. I. Vapor Pressure of Primary n-Alkyl Chlorides and Alcohols. *J. Chem. Eng. Data.* **1969**, *14(1)*, 98-102.

9. ACRONYMS AND NOMENCLATURE

BL	Butyl levulinate
BuOH	1-butanol
CS	Conventionally sulfonated
d_p	Particle diameter, mm
d_{pore}	(macro)pore diameter, mm
DVB	Divinylbenzene
ETBE	Ethyl *tert*-butyl ether
HMF	Hydroxymethyl-furfural
ISEC	Inverse size exclusion chromatography
LA	Levulinic acid
m_{cat}	Catalyst mass
n_j	Mol of species j
OS	Oversulfonated
PS	Polystyrene
$R_{BuOH/LA}$	Molar ratio of butanol versus levulinic acid
S^E_j	Selectivity of reagent j towards product E.
SS	Surface sulfonated
t	time
T	Temperature, ºC, K
T_{max}	Maximum work temperature, ºC, K
V_{sp}	Specific volume of swollen polymer, cm^3/g
X_j	Conversion of reagent j
ΣS_{pore}	Global (macro)pore surface, m^2/g
ΣV_{pore}	Global (macro)pore volume, cm^3/g

APPENDICES

APPENDIX: GC CALIBRATION

Chromatographic analysis is based on a separation technique that carries a sample diluted in a fluid called the *mobile phase* through a structure of another material called the *stationary phase*. Because the different components of a mixture show also different affinity to both the mobile and stationary phase, they travel (elute) at different speeds.

Gas chromatography (GC) is a type of chromatography used in analytical chemistry for separating and analyzing compounds in which the mobile phase is a carrier gas (typically He or another nonreactive gas). The stationary phase is a microscopic layer of liquid or polymer over an inert solid support inside a *packed* or *capillary column*. The vaporized compounds analyzed interact with the walls of the column, each of them elute at different times known as the retention time of the compound. A detector is used to monitor the output stream of the column and makes it possible to determine both retention times and the relative amount of the components (signal intensity). In the same chromatograph, in identical conditions elution times will remain invariable, which is what GC a viable method of analysis. Retention times for components of the system for the esterification of LA with BuOH are specified in Table 10.

Compound		Retention time (min)
nitrogen	N_2	4.348
water	H_2O	4.484
1-butanol	BuOH	6.489
dibutyleter	DBE	9.825
levulinic acid	LA	11.974
butyl levulinate	BL	15.440

Table 10. Retention times for the components of the LA esterification reaction.

Typically chromatographic data is represented as a graph of detector response (y-axis) against retention time (x-axis) called chromatogram. This is a way to visualize the separation of components in different peaks and whether or not they overlap. An appropriate analytical method (variables are running time and oven temperature) will avoid any kind of overlap

between different peaks. The area under each peak is proportional to the amount said component present in a sample. Quantitative analysis by GC is based in the correlation between peak area and sample concentration.
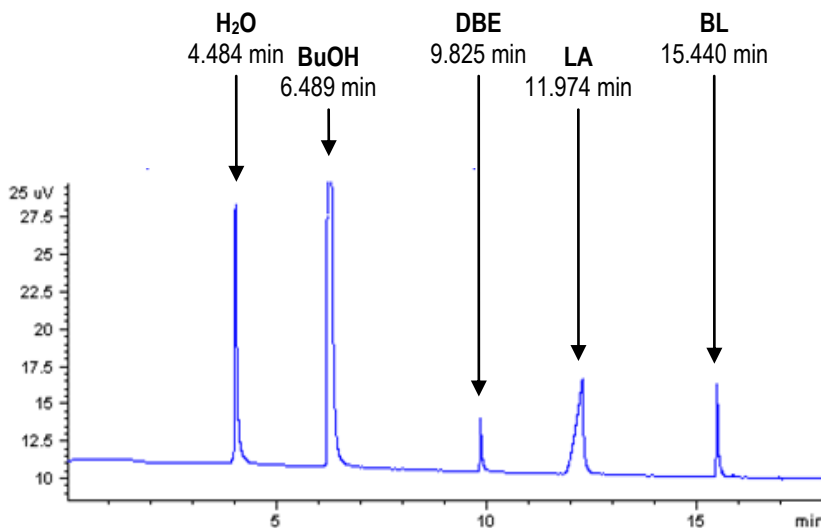
Figure 17.Typical sample chromatogram of the LA esterification system.

In order to relate the percentage of area with the percentage in mass in any given sample it is necessary to first calibrate the system with standards of known composition. This is especially important when some components have very different chemical natures, and their response varies greatly in intensity. In this case this is especially applicable because of the marked differences in polarity and boiling points of the components.

For the study of the esterification of LA with BuOH, 22 vials with known percentage of mass in each component were prepared. They were made to encompass the entire range of concentrations possible in the reaction for all components involved (Table 11). LA and BuOH react at ambient temperature in small quantities. In order to forestall the reaction the calibration vials were kept in ice. Three replicates were performed of the analysis of each vial in order to evaluate statistical dispersion (Tables 13-17).

VIAL	MASS %					VIAL	MASS %				
	H_2O	BuOH	DBE	LA	BL		H_2O	BuOH	DBE	LA	BL
VIAL 1	0.71	85.85	0.00	13.45	0.00	VIAL 12	14.06	54.75	3.28	27.56	0.35
VIAL 2	0.80	74.19	0.09	0.14	24.76	VIAL 13	0.34	68.12	1.28	0.00	30.27
VIAL 3	1.26	74.14	0.26	1.33	23.01	VIAL 14	2.44	56.81	1.04	4.95	34.45
VIAL 4	2.27	74.59	0.17	2.97	19.99	VIAL 15	1.16	79.97	2.21	14.41	2.27
VIAL 5	2.62	74.77	0.26	5.99	16.36	VIAL 16	12.65	44.12	0.64	0.00	42.58
VIAL 6	4.23	75.62	0.13	9.00	11.02	VIAL 17	6.60	36.99	3.55	0.00	52.86
VIAL 7	6.21	72.98	0.45	12.09	8.27	VIAL 18	0.30	60.80	0.00	0.00	38.90
VIAL 8	6.82	71.83	0.75	6.93	13.67	VIAL 19	0.27	55.06	0.00	0.00	44.67
VIAL 9	7.55	67.24	1.44	16.91	6.86	VIAL 20	0.24	49.62	0.00	0.00	50.13
VIAL 10	9.83	62.97	1.99	20.61	4.61	VIAL 21	0.23	46.38	0.00	0.00	53.39
VIAL 11	10.74	59.60	2.68	23.69	3.28	VIAL 22	0.20	41.05	0.00	0.00	58.75

Table 11.Calibration standards for the LA esterification reaction system.

Data points were adjusted to a linear or second order polynomial function by linear or polynomial regression (Table 12). Fisher's test was applied to both linear and polynomial fit in order to ascertain statistical significance.

Component	%MASS = f(%AREA)	R^2
H_2O	%MASS = (0.114 ± 0.110) + (0.877 ± 0.016)·%AREA	0.9983
BuOH	%MASS = (0.818 ± 0.021)·%AREA + (0.0014 ± 0.0001)·%AREA^2	0.9999
DBE	%MASS = (1.169 ± 0.036)·%AREA - (0.048 ± 0.013)·%AREA^2	0.9996
LA	%MASS = (1.700 ± 0.038)·%AREA - (0.017 ± 0.002)·%AREA^2	0.9997
BL	%MASS = (1.288 ± 0.024)·%AREA - (0.003 ± 0.001)·%AREA^2	0.9998

Table 12. Calibration curves for all the components of the LA esterification reaction system.
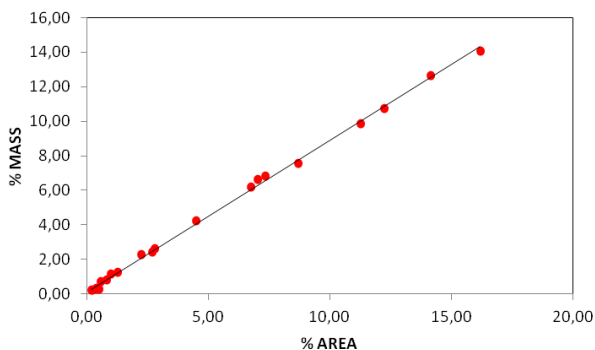
VIAL	MASS %	AREA 1 (%)	AREA 2 (%)	AREA 3 (%)	AV. AREA (%)
1	0.71	0.36	0.57	0.79	0.58 ± 0.24
2	0.80	0.76	0.77	0.88	0.80 ± 0.08
3	1.26	1.06	1.13	1.58	1.26 ± 0.16
4	2.27	2.22	2.28	2.20	2.23 ± 0.04
5	2.62	2.69	5.89	2.80	2.79 ± 0.12
6	4.23	4.47	4.45	4.55	4.49 ± 0.06
7	6.21	7.22	6.58	6.47	6.75 ± 0.46
8	6.82	7.51	7.15	7.31	7.32 ± 0.21
9	7.55	9.62	8.10	8.36	8.69 ± 0.92
10	9.83	10.85	11.24	11.66	11.25 ± 0.46
11	10.74	12.04	12.31	12.37	12.24 ± 0.20
12	14.06	15.99	16.18	16.39	16.18 ± 0.22
13	0.34	0.15	0.34	0.66	0.38 ± 0.29
14	2.44	2.50	2.73	2.81	2.68 ± 0.18
15	1.16	0.72	0.96	1.27	0.98 ± 0.31
16	12.65	13.57	14.17	14.66	14.14 ± 0.62
17	6.60	6.59	6.98	7.52	7.03 ± 0.53
18	0.30	0.35	0.38	0.50	0.41 ± 0.09
19	0.27	0.21	0.38	0.56	0.38 ± 0.20
20	0.24	0.23	0.55	0.68	0.49 ± 0.26
21	0.23	0.24	0.23	0.22	0.23 ± 0.01
22	0.20	0.16	0.16	0.20	0.17 ± 0.03

Table 13.Calibration data and linear fit for water in the LA esterification reaction system.
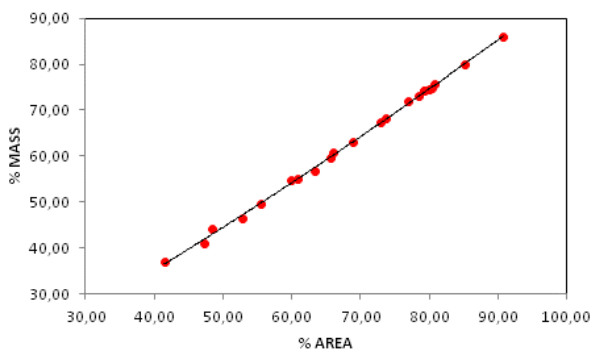
VIAL	MASS %	AREA 1 (%)	AREA 2 (%)	AREA 3 (%)	AV. AREA (%)
1	85.85	90.30	90.97	91.06	90.78 ± 0.47
2	74.19	79.44	79.63	78.63	79.24 ± 0.58
3	74.14	78.08	80.11	79.42	79.20 ± 1.17
4	74.59	79.56	80.36	80.17	80.03 ± 0.47
5	74.77	79.98	81.29	79.87	80.38 ± 0.90
6	75.62	80..45	80.78	80.97	80.73 ± 0.30
7	72.98	77.80	79.45	78.35	78.53 ± 0.95
8	71.83	76.99	77.10	77.00	77.03 ± 0.07
9	67.24	72.43	73.23	73.27	72.98 ± 0.53
10	62.97	68.81	68.83	68.94	68.86 ± 0.08
11	59.60	65.34	66.54	65.29	65.73 ± 0.80
12	54.75	59.11	59.90	60.58	59.86 ± 0.83
13	68.12	72.90	74.26	73.73	73.63 ± 0.77
14	56.81	63.19	63.75	63.31	63.41 ± 0.34
15	79.97	85.10	85.43	85.11	85.21 ± 0.21
16	44.12	48.43	49.11	48.05	48.53 ± 0.61
17	36.99	40.58	41.84	41.98	41.46 ± 0.88
18	60.80	66.44	65.18	66.35	65.99 ± 0.80
19	55.06	60.70	61.48	60.52	60.90 ± 0.58
20	49.62	55.73	56.59	54.15	55.49 ± 1.40
21	46.38	51.95	53.49	53.28	52.91 ± 0.95
22	41.05	48.15	46.86	46.85	47.29 ± 0.84

Table 14.Calibration data and linear fit for BuOH in the LA esterification reaction system.
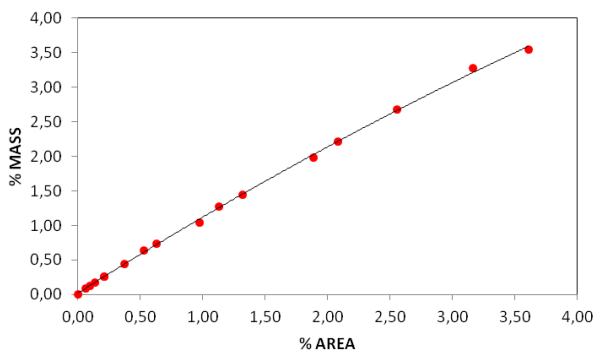
VIAL	MASS %	AREA 1 (%)	AREA 2 (%)	AREA 3 (%)	AV. AREA (%)
1	0.00	0.00	0.00	0.00	0.00 ± 0.00
2	0.09	0.07	0.06	0.06	0.06 ± 0.01
3	0.26	0.21	0.22	0.21	0.21 ± 0.01
4	0.17	0.15	0.14	0.11	0.13 ± 0.02
5	0.26	0.22	0.21	0.20	0.21 ± 0.02
6	0.13	0.11	0.09	0.09	0.10 ± 0.01
7	0.45	0.37	0.37	0.37	0.37 ± 0.00
8	0.75	0.62	0.66	0.61	0.63 ± 0.03
9	1.44	1.27	1.36	1.33	1.32 ± 0.05
10	1.99	1.94	1.83	1.87	1.88 ± 0.06
11	2.68	2.58	2.59	2.49	2.56 ± 0.07
12	3.28	3.12	3.12	3.24	3.16 ± 0.08
13	1.28	1.18	1.13	1.08	1.13 ± 0.05
14	1.04	0.97	1.00	0.95	0.97 ± 0.03
15	2.21	2.16	2.01	2.07	2.08 ± 0.08
16	0.64	0.52	0.54	0.52	0.53 ± 0.01
17	3.55	3.54	3.62	3.66	3.61 ± 0.07

Table 15.Calibration data and linear fit for DBE in the LA esterification reaction system.
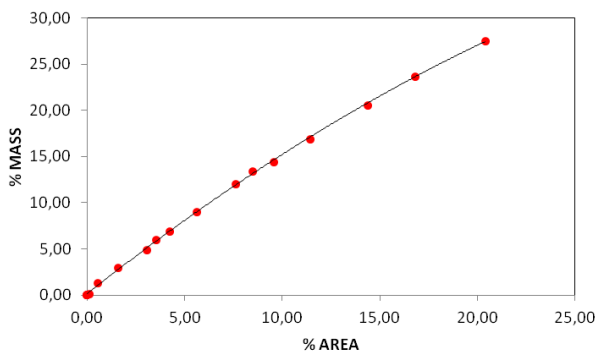
VIAL	MASS %	AREA 1 (%)	AREA 2 (%)	AREA 3 (%)	AV. AREA (%)
1	13,45	9.19	8.31	8.00	8,50 ± 0.70
2	0,14	0.14	0.08	0.08	0,10 ± 0.04
3	1,33	0.61	0.49	0.59	0,56 ± 0.07
4	2,97	1.64	1.52	1.61	1,59 ± 0.07
5	5,99	3.66	3.32	3.67	3,55 ± 0.23
6	9,00	5.80	5.52	5.48	5,60 ± 0.20
7	12,09	7.81	7.03	7.96	7,60 ± 0.56
8	6,93	4.20	4.25	4.20	4,22 ± 0.03
9	16,91	11.19	11.11	12.02	11,44 ± 0.57
10	20,61	14.73	14.47	13.95	14,38 ± 0.45
11	23,69	17.25	15.92	17.21	16,79 ± 0.86
12	27,56	21.37	20.41	19.39	20,39 ± 1.12
13	0,00	0.00	0.00	0.00	0,00 ± 0.00
14	4,95	2.97	2.98	3.18	3,04 ± 0.14
15	14,41	10.16	9.26	9.32	9,58 ± 0.57

Table 16.Calibration data and linear fit for LA in the LA esterification reaction system.
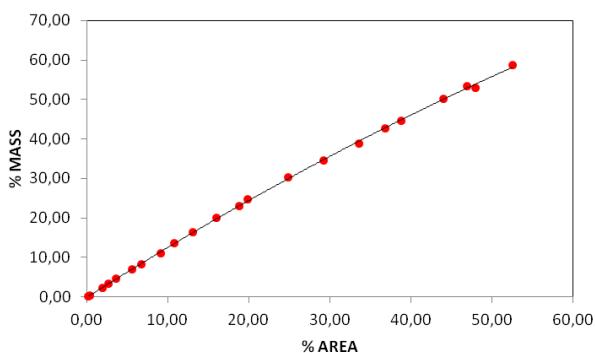
VIAL	MASS %	AREA 1 (%)	AREA 2 (%)	AREA 3 (%)	AV. AREA (%)
1	0.00	0.15	0.14	0.15	0.15 ± 0.01
2	24.76	19.58	19.46	20.33	19.79 ± 0.53
3	23.01	19.95	17.85	18.44	18.75 ± 1.22
4	19.99	16.43	15.70	15.91	16.02 ± 16.02
5	16.36	13.45	12.29	13.47	13.07 ± 0.77
6	11.02	9.18	9.16	8.92	9.08 ± 0.16
7	8.27	6.80	6.58	6.86	6.75 ± 0.17
8	13.67	10.67	10.84	10.90	10.80 ± 0.13
9	6.86	5.48	5.36	5.91	5.58 ± 0.33
10	4.61	4.03	3.49	3.34	3.62 ± 0.41
11	3.28	2.78	2.64	2.64	2.69 ± 0.09
12	0.35	0.41	0.40	0.40	0.40 ± 0.01
13	30.27	24.93	24.77	24.87	24.86 ± 0.09
14	34.45	29.12	29.12	29.19	29.14 ± 0.05
15	2.27	2.12	1.68	1.90	1.90 ± 0.25
16	42.58	37.48	36.18	36.76	36.81 ± 0.74
17	52.86	49.29	47.57	46.84	47.90 ± 1.43
18	38.90	33.20	34.44	33.15	33.60 ± 0.83
19	44.67	39.09	38.13	38.93	38.72 ± 0.58
20	50.13	44.03	42.86	45.17	44.02 ± 1.31
21	53.39	45.53	46.04	46.35	46.87 ± 0.47
22	58.75	51.70	52.98	52.94	52.54 ± 0.82

Table 17.Calibration data and linear fit for BL in the LA esterification reaction system.

APPENDIX 2: EXPERIMENTAL DATA

The data obtained from the monitoring of every experiment undertaken and deemed relevant to this study have been included in this section. The following pertain to preliminary experiments 1-11 (Table 18-28), and the catalyst screening experiments 1-12 (Table 29-40).

Preliminary Experiment 1			T	100 ºC	m_{BuOH}	48,42 g	n_{BuOH}	0,653 mol
			$R_{BuOH/LA}$	7	m_{LA}	10,63 g	n_{LA}	0,092 mol
Catalyst	Amberlyst 39		m_{cat}	1,077 g	m_{H2O}	0,46 g	n_{H2O}	0,026 mol

t	$\dfrac{w \cdot t}{n^o_{LA}}$	AREA (%)					n_j (mol)					X_{LA} (%)	SELECTIVITY	
		H_2O	BuOH	DBE	LA	BL	H_2O	BuOH	DBE	LA	BL		S^{BL}_{BuOH}	S^{DBE}_{BuOH}
0	0,00	1,22	88,81	0,64	6,91	2,42	0,039	0,675	0,003	0,056	0,011	16,09	61,68	19,16
1	11,71	2,06	79,55	0,11	1,85	16,43	0,063	0,596	0,001	0,016	0,070	81,54	98,32	0,84
2	23,43	2,08	78,88	0,02	0,46	18,57	0,064	0,590	0,000	0,004	0,079	95,21	99,73	0,13
3	35,14	2,01	78,22	0,04	0,20	19,53	0,062	0,585	0,000	0,002	0,082	97,94	99,49	0,26
4	46,85	1,99	78,04	0,06	0,16	19,75	0,062	0,583	0,000	0,001	0,083	98,38	99,25	0,38
5	58,57	1,88	77,68	0,06	0,10	20,28	0,058	0,580	0,000	0,001	0,085	99,00	99,26	0,37
6	70,28	2,03	75,52	0,07	0,09	22,28	0,063	0,562	0,000	0,001	0,093	99,14	99,16	0,42
7	81,99	1,78	77,47	0,08	0,10	20,57	0,055	0,578	0,000	0,001	0,087	99,01	99,03	0,48
8	93,70	1,95	75,08	0,11	0,09	22,76	0,060	0,558	0,001	0,001	0,095	99,16	98,77	0,62

Table 18. Data corresponding to Preliminary Experiment 1.

Preliminary Experiment 2			T	120 ºC	m$_{BuOH}$	48,73 g	n$_{BuOH}$	0,657 mol
			R$_{BuOH/LA}$	7	m$_{LA}$	10,93 g	n$_{LA}$	0,094 mol
Catalyst	Amberlyst 39		m$_{cat}$	1,005 g	m$_{H2O}$	0,47 g	n$_{H2O}$	0,026 mol

t	$\dfrac{w \cdot t}{n_{LA}^{o}}$	AREA (%)					n$_j$ (mol)					X$_{LA}$ (%)	SELECTIVITY	
		H$_2$O	BuOH	DBE	LA	BL	H$_2$O	BuOH	DBE	LA	BL		S$_{BuOH}^{BL}$	S$_{BuOH}^{DBE}$
0	0,00	1,09	87,28	0,57	5,96	5,09	0,036	0,668	0,003	0,049	0,023	31,42	78,85	10,57
1	10,93	1,95	78,84	0,10	0,89	18,22	0,061	0,595	0,001	0,008	0,078	90,98	98,63	0,68
2	21,86	1,91	77,38	0,18	0,34	20,19	0,060	0,583	0,001	0,003	0,086	96,66	97,82	1,09
3	32,79	1,89	77,16	0,28	0,12	20,55	0,059	0,581	0,001	0,001	0,087	98,82	96,71	1,64
4	43,72	1,81	76,66	0,36	0,10	21,07	0,057	0,577	0,002	0,001	0,089	99,02	95,88	2,06
5	54,65	1,83	76,49	0,36	0,12	21,20	0,057	0,576	0,002	0,001	0,090	98,84	95,90	2,05
6	65,58	1,70	76,44	0,60	0,08	21,19	0,053	0,575	0,003	0,001	0,090	99,23	93,45	3,28
7	76,51	1,57	75,86	0,72	0,08	21,78	0,050	0,570	0,004	0,001	0,092	99,25	92,47	3,76
8	87,44	1,51	75,96	0,83	0,06	21,64	0,048	0,571	0,004	0,001	0,092	99,42	91,41	4,29

Table 19. Data corresponding to Preliminary Experiment 2.

Preliminary Experiment 3			T	80 ºC	m$_{BuOH}$	48,82 g	n$_{BuOH}$	0,659 mol
			R$_{BuOH/LA}$	7	m$_{LA}$	10,93 g	n$_{LA}$	0,094 mol
Catalyst	Amberlyst 39		m$_{cat}$	1,046 g	m$_{H2O}$	0,47 g	n$_{H2O}$	0,026 mol

t	$\dfrac{w \cdot t}{n_{LA}^{o}}$	AREA (%)					n$_j$ (mol)					X$_{LA}$ (%)	SELECTIVITY	
		H$_2$O	BuOH	DBE	LA	BL	H$_2$O	BuOH	DBE	LA	BL		S$_{BuOH}^{BL}$	S$_{BuOH}^{DBE}$
0	0,00	1,06	89,05	0,56	6,06	3,28	0,035	0,683	0,003	0,050	0,015	22,61	71,24	14,38
2	22,75	1,98	79,69	0,17	2,15	16,01	0,062	0,604	0,001	0,019	0,069	78,81	97,47	1,27
3	34,13	1,90	80,38	0,04	0,99	16,69	0,060	0,609	0,000	0,009	0,072	89,26	99,41	0,30
4	45,50	1,86	79,19	0,04	0,69	18,22	0,058	0,599	0,000	0,006	0,078	92,80	99,46	0,27
5	56,88	2,12	76,90	0,04	0,43	20,51	0,066	0,580	0,000	0,004	0,087	95,87	99,54	0,23
6	68,26	1,91	78,68	0,02	0,26	19,13	0,060	0,595	0,000	0,002	0,082	97,32	99,74	0,13
7	79,63	1,89	78,64	0,02	0,18	19,27	0,059	0,595	0,000	0,002	0,082	98,13	99,74	0,13
8	91,01	1,89	78,31	0,02	0,16	19,63	0,059	0,592	0,000	0,001	0,084	98,38	99,75	0,13

Table 20. Data corresponding to Preliminary Experiment 3.

Preliminary Experiment 4		**T**	**120 ºC**	**m$_{BuOH}$**	46,14 g	**n$_{BuOH}$**	0,623 mol
		R$_{BuOH/LA}$	**5**	**m$_{LA}$**	14,43 g	**n$_{LA}$**	0,124 mol
Catalyst	**Amberlyst 39**	**m$_{cat}$**	**1,021 g**	**m$_{H2O}$**	0,53 g	**n$_{H2O}$**	0,029 mol

t	$\dfrac{w \cdot t}{n_{LA}^o}$	AREA (%)					n$_j$ (mol)					X$_{LA}$ (%)	SELECTIVITY	
		H$_2$O	BuOH	DBE	LA	BL	H$_2$O	BuOH	DBE	LA	BL		S$_{BuOH}^{BL}$	S$_{BuOH}^{DBE}$
0	0,00	1,27	85,74	0,33	8,56	4,11	0,042	0,665	0,002	0,070	0,019	20,99	83,99	8,01
1	11,10	2,57	71,92	0,06	1,47	23,99	0,080	0,546	0,000	0,013	0,103	88,78	99,37	0,32
2	22,21	2,56	69,65	0,12	0,91	26,76	0,080	0,527	0,001	0,008	0,114	93,35	98,87	0,57
3	33,31	2,54	69,34	0,20	0,41	27,51	0,079	0,524	0,001	0,004	0,117	96,94	98,20	0,90
4	44,42	2,47	69,18	0,26	0,30	27,79	0,077	0,523	0,001	0,003	0,118	97,79	97,67	1,17
5	55,52	2,36	68,77	0,38	0,30	28,19	0,074	0,520	0,002	0,003	0,119	97,82	96,70	1,65
6	66,62	2,25	68,79	0,40	0,28	28,29	0,071	0,520	0,002	0,002	0,120	97,98	96,56	1,72
7	77,73	2,25	68,43	0,45	0,24	28,63	0,071	0,517	0,002	0,002	0,121	98,28	96,11	1,95
8	88,83	2,15	68,03	0,56	0,24	29,03	0,068	0,513	0,003	0,002	0,122	98,29	95,35	2,33

Table 21. Data corresponding to Preliminary Experiment 4.

Preliminary Experiment 5		**T**	**120 ºC**	**m$_{BuOH}$**	50,45 g	**n$_{BuOH}$**	0,681 mol
		R$_{BuOH/LA}$	**9**	**m$_{LA}$**	8,88 g	**n$_{LA}$**	0,077 mol
Catalyst	**Amberlyst 39**	**m$_{cat}$**	**1,016 g**	**m$_{H2O}$**	0,43 g	**n$_{H2O}$**	0,024 mol

t	$\dfrac{w \cdot t}{n_{LA}^o}$	AREA (%)					n$_j$ (mol)					X$_{LA}$ (%)	SELECTIVITY	
		H$_2$O	BuOH	DBE	LA	BL	H$_2$O	BuOH	DBE	LA	BL		S$_{BuOH}^{BL}$	S$_{BuOH}^{DBE}$
0	0,00	0,87	91,11	0,49	4,48	3,04	0,029	0,695	0,003	0,037	0,013	26,47	72,18	13,91
1	11,05	1,91	81,68	0,09	0,66	15,65	0,059	0,616	0,000	0,006	0,067	92,10	98,56	0,72
2	22,10	1,66	80,65	0,21	0,09	17,40	0,052	0,607	0,001	0,001	0,074	98,90	97,12	1,44
3	33,15	1,55	80,33	0,33	0,06	17,73	0,049	0,604	0,002	0,001	0,076	99,34	95,64	2,18
4	44,20	1,66	79,68	0,41	0,06	18,20	0,052	0,599	0,002	0,000	0,077	99,37	94,70	2,65
5	55,25	1,39	80,08	0,55	0,04	17,94	0,044	0,602	0,003	0,000	0,076	99,57	92,96	3,52
6	66,30	1,31	80,14	0,68	0,02	17,85	0,042	0,603	0,004	0,000	0,076	99,78	91,51	4,25
7	77,35	1,60	78,84	0,82	0,04	18,71	0,050	0,592	0,004	0,000	0,079	99,59	90,37	4,82
8	88,40	1,49	78,55	0,98	0,04	18,94	0,047	0,590	0,005	0,000	0,080	99,60	88,80	5,60

Table 22. Data corresponding to Preliminary Experiment 5.

Preliminary Experiment 6		T	120 ºC	m_{BuOH}	41,56 g	n_{BuOH}	0,561 mol
		$R_{BuOH/LA}$	3	m_{LA}	21,49 g	n_{LA}	0,185 mol
Catalyst	Amberlyst 39	m_{cat}	1,084 g	m_{H2O}	0,65 g	n_{H2O}	0,036 mol

t	$\dfrac{w \cdot t}{n_{LA}^{o}}$	AREA (%)					n_j (mol)					X_{LA} (%)	SELECTIVITY	
		H_2O	BuOH	DBE	LA	BL	H_2O	BuOH	DBE	LA	BL		S_{BuOH}^{BL}	S_{BuOH}^{DBE}
0	0,00	0,93	78,84	0,73	17,32	2,18	0,033	0,631	0,004	0,133	0,010	7,20	56,15	21,93
1	11,79	3,86	55,50	0,04	3,03	37,57	0,124	0,428	0,000	0,027	0,161	85,46	99,72	0,14
2	23,58	3,81	53,20	0,06	1,73	41,20	0,122	0,409	0,000	0,016	0,175	91,70	99,61	0,20
3	35,37	3,62	52,52	0,12	1,46	42,27	0,116	0,403	0,001	0,013	0,179	93,00	99,25	0,38
4	47,16	3,49	51,99	0,12	1,34	43,07	0,112	0,399	0,001	0,012	0,182	93,66	99,26	0,37
5	58,95	3,42	51,89	0,14	1,25	43,29	0,110	0,398	0,001	0,012	0,183	94,05	99,13	0,44
6	70,74	3,24	51,49	0,18	1,21	43,88	0,105	0,395	0,001	0,011	0,185	94,30	98,91	0,54
7	82,52	3,11	50,88	0,18	1,11	44,72	0,100	0,390	0,001	0,010	0,188	94,83	98,91	0,54
8	94,31	3,03	50,66	0,24	1,07	45,00	0,098	0,388	0,001	0,010	0,189	95,05	98,57	0,71

Table 23. Data corresponding to Preliminary Experiment 6.

Preliminary Experiment 7		T	80 ºC	m_{BuOH}	41,22 g	n_{BuOH}	0,556 mol
		$R_{BuOH/LA}$	3	m_{LA}	21,74 g	n_{LA}	0,187 mol
Catalyst	-	m_{cat}	-	m_{H2O}	0,65 g	n_{H2O}	0,036 mol

t	$\dfrac{w \cdot t}{n_{LA}^{o}}$	AREA (%)					n_j (mol)					X_{LA} (%)	SELECTIVITY	
		H_2O	BuOH	DBE	LA	BL	H_2O	BuOH	DBE	LA	BL		S_{BuOH}^{BL}	S_{BuOH}^{DBE}
0	-	1,32	80,34	0,13	15,08	3,14	0,045	0,643	0,001	0,119	0,015	11,09	91,21	4,40
1	-	1,31	77,97	0,12	16,54	4,06	0,045	0,622	0,001	0,128	0,019	13,00	93,21	3,39
2	-	1,38	76,62	0,10	16,79	5,10	0,047	0,610	0,001	0,129	0,024	15,60	95,32	2,34
3	-	1,45	76,53	0,08	16,86	5,08	0,049	0,609	0,000	0,130	0,024	15,51	96,20	1,90
4	-	1,41	75,54	0,10	17,13	5,82	0,048	0,601	0,001	0,132	0,027	17,18	95,91	2,04
5	-	1,41	75,41	0,08	16,70	6,40	0,048	0,599	0,000	0,129	0,030	18,83	96,94	1,53
6	-	1,52	75,26	0,10	16,22	6,90	0,051	0,598	0,001	0,126	0,032	20,36	96,49	1,75
8	-	1,50	73,25	0,10	16,67	8,48	0,051	0,580	0,001	0,129	0,039	23,44	97,15	1,43

Table 24. Data corresponding to Preliminary Experiment 7.

Preliminary Experiment 8		T	120 ºC	m_{BuOH}	41,65 g	n_{BuOH}	0,562 mol
		$R_{BuOH/LA}$	3	m_{LA}	22,61 g	n_{LA}	0,195 mol
Catalyst	Amberlyst 39	m_{cat}	1,013 g	m_{H2O}	0,67 g	n_{H2O}	0,037 mol

t	$\dfrac{w \cdot t}{n_{LA}^{o}}$	AREA (%)					n_j (mol)					X_{LA} (%)	SELECTIVITY	
		H_2O	BuOH	DBE	LA	BL	H_2O	BuOH	DBE	LA	BL		S_{BuOH}^{BL}	S_{BuOH}^{DBE}
0	0,00	1,56	75,86	0,09	16,97	5,53	0,054	0,616	0,000	0,133	0,026	16,56	96,37	1,81
1	5,20	3,41	56,40	0,04	4,33	35,82	0,112	0,444	0,000	0,039	0,157	79,99	99,70	0,15
2	10,41	3,54	51,80	0,06	1,77	42,82	0,116	0,405	0,000	0,017	0,184	91,77	99,62	0,19
3	15,61	3,42	51,29	0,10	1,37	43,83	0,112	0,401	0,001	0,013	0,188	93,62	99,38	0,31
4	20,81	3,31	50,94	0,16	1,24	44,35	0,109	0,398	0,001	0,012	0,190	94,24	99,02	0,49
5	26,01	3,25	50,76	0,20	1,22	44,56	0,107	0,396	0,001	0,011	0,191	94,32	98,80	0,60
6	31,22	3,11	50,39	0,20	1,12	45,19	0,102	0,393	0,001	0,010	0,193	94,85	98,80	0,60
8	36,42	3,11	50,39	0,28	1,12	45,10	0,102	0,393	0,002	0,011	0,193	94,81	98,35	0,82

Table 25. Data corresponding to Preliminary Experiment 8.

Preliminary Experiment 9		T	120 ºC	m_{BuOH}	41,22 g	n_{BuOH}	0,556 mol
		$R_{BuOH/LA}$	3	m_{LA}	21,39 g	n_{LA}	0,184 mol
Catalyst	Amberlyst 15	m_{cat}	1,015 g	m_{H2O}	0,64 g	n_{H2O}	0,036 mol

t	$\dfrac{w \cdot t}{n_{LA}^{o}}$	AREA (%)					n_j (mol)					X_{LA} (%)	SELECTIVITY	
		H_2O	BuOH	DBE	LA	BL	H_2O	BuOH	DBE	LA	BL		S_{BuOH}^{BL}	S_{BuOH}^{DBE}
0	0,00	1,56	75,86	0,09	16,97	5,53	0,052	0,600	0,000	0,130	0,026	16,56	96,37	1,81
1	5,51	3,50	56,23	0,04	3,93	36,30	0,112	0,431	0,000	0,035	0,155	81,64	99,71	0,15
2	11,02	3,65	53,28	0,08	1,69	41,30	0,117	0,407	0,000	0,015	0,174	91,85	99,48	0,26
3	16,53	3,55	52,61	0,08	1,28	42,48	0,113	0,401	0,000	0,012	0,178	93,83	99,49	0,25
4	22,04	3,41	52,44	0,10	1,18	42,87	0,109	0,400	0,001	0,011	0,180	94,32	99,37	0,31
5	27,55	3,24	52,23	0,12	1,14	43,28	0,104	0,398	0,001	0,010	0,181	94,56	99,26	0,37
6	33,05	3,20	51,93	0,14	1,05	43,68	0,103	0,396	0,001	0,010	0,183	95,01	99,14	0,43
8	38,56	3,08	51,68	0,16	1,03	44,04	0,099	0,393	0,001	0,009	0,184	95,10	99,03	0,48

Table 26. Data corresponding to Preliminary Experiment 8.

Preliminary Experiment 10			T	120 ºC	m_{BuOH}	41,26 g	n_{BuOH}	0,557 mol
			$R_{BuOH/LA}$	3	m_{LA}	21,94 g	n_{LA}	0,189 mol
Catalyst	Amberlyst 16		m_{cat}	1,026 g	m_{H2O}	0,66 g	n_{H2O}	0,036 mol

t	$\dfrac{w \cdot t}{n_{LA}^{o}}$	AREA (%)					n_j (mol)					X_{LA} (%)	SELECTIVITY	
		H_2O	BuOH	DBE	LA	BL	H_2O	BuOH	DBE	LA	BL		S_{BuOH}^{BL}	S_{BuOH}^{DBE}
0	0,00	1,56	75,86	0,09	16,97	5,53	0,053	0,606	0,000	0,131	0,026	16,56	96,37	1,81
1	5,43	3,54	56,37	0,06	4,15	35,88	0,114	0,436	0,000	0,037	0,155	80,68	99,56	0,22
2	10,86	3,77	52,96	0,08	1,79	41,39	0,121	0,408	0,000	0,016	0,176	91,44	99,48	0,26
3	16,29	3,63	52,29	0,12	1,40	42,56	0,117	0,402	0,001	0,013	0,180	93,34	99,25	0,38
4	21,72	3,42	52,02	0,14	1,24	43,17	0,111	0,400	0,001	0,011	0,183	94,09	99,13	0,43
5	27,15	3,37	51,73	0,16	1,19	43,55	0,109	0,398	0,001	0,011	0,184	94,38	99,01	0,49
6	32,58	3,22	51,21	0,20	1,11	44,26	0,104	0,393	0,001	0,010	0,186	94,77	98,78	0,61
8	38,01	3,05	50,81	0,24	1,13	44,76	0,099	0,390	0,001	0,010	0,188	94,74	98,56	0,72

Table 27. Data corresponding to Preliminary Experiment 10.

Preliminary Experiment 11			T	120 ºC	m_{BuOH}	41,55 g	n_{BuOH}	0,561 mol
			$R_{BuOH/LA}$	3	m_{LA}	22,32 g	n_{LA}	0,192 mol
Catalyst	Dowex 50Wx8		m_{cat}	1,088 g	m_{H2O}	0,66 g	n_{H2O}	0,037 mol

t	$\dfrac{w \cdot t}{n_{LA}^{o}}$	AREA (%)					n_j (mol)					X_{LA} (%)	SELECTIVITY	
		H_2O	BuOH	DBE	LA	BL	H_2O	BuOH	DBE	LA	BL		S_{BuOH}^{BL}	S_{BuOH}^{DBE}
0	97,01	1,57	75,36	0,06	18,15	4,86	0,053	0,608	0,000	0,140	0,023	14,23	97,01	1,50
1	99,59	3,58	54,36	0,06	3,52	38,48	0,117	0,424	0,000	0,032	0,167	83,88	99,59	0,21
2	99,49	3,65	51,66	0,08	1,81	42,80	0,119	0,401	0,000	0,017	0,183	91,59	99,49	0,25
3	99,38	3,47	51,02	0,10	1,46	43,95	0,113	0,396	0,001	0,014	0,187	93,23	99,38	0,31
4	99,03	3,36	51,05	0,16	1,37	44,05	0,110	0,396	0,001	0,013	0,188	93,62	99,03	0,48
5	98,91	3,29	50,81	0,18	1,30	44,41	0,108	0,394	0,001	0,012	0,189	93,96	98,91	0,54
6	98,81	3,14	50,51	0,20	1,16	44,99	0,103	0,392	0,001	0,011	0,191	94,64	98,81	0,59
8	98,83	3,96	50,97	0,19	0,68	44,21	0,129	0,395	0,001	0,006	0,188	96,74	98,83	0,58

Table 28. Data corresponding to Preliminary Experiment 11.

Screening Exp. 1		T	80 ºC	m_{BuOH}	41,57 g	n_{BuOH}	0,561 mol
		$R_{BuOH/LA}$	3	m_{LA}	22,35 g	n_{LA}	0,193 mol
Catalyst	Dowex 50Wx2	m_{cat}	1,009 g	m_{H2O}	0,67 g	n_{H2O}	0,037 mol

t	$\dfrac{w \cdot t}{n_{LA}^{o}}$	AREA (%)					n_j (mol)					X_{LA} (%)	SELECTIVITY	
		H_2O	BuOH	DBE	LA	BL	H_2O	BuOH	DBE	LA	BL		S_{BuOH}^{BL}	S_{BuOH}^{DBE}
0	0,00	1,54	74,72	0,09	15,80	7,86	0,052	0,602	0,000	0,125	0,037	22,88	97,41	1,29
1	5,24	2,61	60,38	0,02	6,38	30,60	0,086	0,476	0,000	0,056	0,136	70,66	99,82	0,09
2	10,48	3,05	54,91	0,02	2,99	39,02	0,100	0,429	0,000	0,027	0,169	86,03	99,86	0,07
3	15,72	2,83	53,99	0,02	1,64	41,52	0,093	0,421	0,000	0,015	0,178	92,14	99,87	0,07
4	20,96	2,73	53,43	0,02	1,33	42,49	0,090	0,417	0,000	0,012	0,182	93,61	99,87	0,07
5	26,20	2,92	53,32	0,02	1,22	42,53	0,096	0,416	0,000	0,011	0,182	94,14	99,87	0,06
6	31,44	2,53	52,91	0,02	1,11	43,44	0,084	0,412	0,000	0,010	0,186	94,71	99,87	0,06
7	36,68	2,38	53,09	0,02	1,02	43,49	0,079	0,414	0,000	0,010	0,186	95,10	99,87	0,07
8	41,93	2,36	52,95	0,02	0,99	43,68	0,078	0,413	0,000	0,009	0,187	95,26	99,87	0,06

Table 29. Data corresponding to Screening Experiment 1.

Screening Exp. 2		T	80 ºC	m_{BuOH}	41,38 g	n_{BuOH}	0,558 mol
		$R_{BuOH/LA}$	3	m_{LA}	22,09 g	n_{LA}	0,190 mol
Catalyst	Amberlyst 39	m_{cat}	0,526 g	m_{H2O}	0,66 g	n_{H2O}	0,037 mol

t	$\dfrac{w \cdot t}{n_{LA}^{o}}$	AREA (%)					n_j (mol)					X_{LA} (%)	SELECTIVITY	
		H_2O	BuOH	DBE	LA	BL	H_2O	BuOH	DBE	LA	BL		S_{BuOH}^{BL}	S_{BuOH}^{DBE}
0	0,00	1,39	77,54	0,09	15,68	5,31	0,048	0,623	0,000	0,124	0,025	16,88	96,17	1,91
1	2,76	1,95	69,11	0,08	12,98	15,88	0,065	0,548	0,000	0,106	0,073	40,83	98,73	0,64
2	5,53	2,53	64,97	0,06	9,88	22,56	0,083	0,512	0,000	0,083	0,102	54,94	99,31	0,34
3	8,29	2,76	62,03	0,02	7,70	27,49	0,090	0,487	0,000	0,067	0,122	64,72	99,81	0,10
4	11,06	2,82	59,78	0,02	6,03	31,36	0,092	0,467	0,000	0,053	0,138	72,20	99,83	0,09
5	13,82	3,36	58,61	0,02	5,02	32,98	0,109	0,457	0,000	0,045	0,144	76,36	99,84	0,08
6	16,59	3,43	57,34	0,02	4,04	35,17	0,111	0,447	0,000	0,036	0,153	80,80	99,85	0,08
7	19,35	3,10	56,65	0,02	3,26	36,98	0,101	0,441	0,000	0,030	0,160	84,40	99,85	0,07
8	22,12	3,04	55,88	0,02	2,80	38,27	0,099	0,434	0,000	0,025	0,165	86,61	99,86	0,07

Table 30. Data corresponding to Screening Experiment 2.

Screening Exp. 3		T	80 ºC	m_{BuOH}	41,52 g	n_{BuOH}	0,560 mol
		$R_{BuOH/LA}$	3	m_{LA}	21,87 g	n_{LA}	0,188 mol
Catalyst	Dowex 50Wx8	m_{cat}	0,514 g	m_{H2O}	0,66 g	n_{H2O}	0,036 mol

t	$\dfrac{w \cdot t}{n_{LA}^o}$	AREA (%)					n_j (mol)					X_{LA} (%)	SELECTIVITY	
		H_2O	BuOH	DBE	LA	BL	H_2O	BuOH	DBE	LA	BL		S_{BuOH}^{BL}	S_{BuOH}^{DBE}
0	0,00	1,37	77,42	0,08	15,52	5,60	0,047	0,622	0,000	0,122	0,026	17,76	96,48	1,76
2	5,46	2,10	66,69	0,08	11,56	19,57	0,070	0,526	0,000	0,096	0,089	48,19	98,96	0,52
3	8,19	2,53	64,82	0,06	9,69	22,90	0,083	0,510	0,000	0,082	0,103	55,73	99,33	0,34
4	10,91	2,51	62,59	0,06	8,02	26,82	0,082	0,491	0,000	0,069	0,119	63,34	99,42	0,29
5	13,64	2,60	60,98	0,02	6,67	29,72	0,085	0,477	0,000	0,058	0,131	69,22	99,82	0,09
6	16,37	2,69	59,17	0,02	5,69	32,43	0,088	0,462	0,000	0,050	0,142	73,87	99,83	0,08
7	19,10	2,85	58,55	0,02	4,65	33,93	0,093	0,456	0,000	0,042	0,148	78,06	99,84	0,08
8	21,83	2,86	57,95	0,04	3,92	35,23	0,093	0,451	0,000	0,035	0,153	81,26	99,70	0,15

Table 31. Data corresponding to Screening Experiment 3.

Screening Exp. 4		T	80 ºC	m_{BuOH}	41,70 g	n_{BuOH}	0,563 mol
		$R_{BuOH/LA}$	3	m_{LA}	22,00 g	n_{LA}	0,189 mol
Catalyst	Dowex 50Wx4	m_{cat}	0,524 g	m_{H2O}	0,66 g	n_{H2O}	0,037 mol

t	$\dfrac{w \cdot t}{n_{LA}^o}$	AREA (%)					n_j (mol)					X_{LA} (%)	SELECTIVITY	
		H_2O	BuOH	DBE	LA	BL	H_2O	BuOH	DBE	LA	BL		S_{BuOH}^{BL}	S_{BuOH}^{DBE}
0	0,00	1,26	76,49	0,09	16,65	5,51	0,044	0,616	0,000	0,130	0,026	16,73	96,37	1,81
1	2,77	1,78	68,47	0,08	11,64	18,02	0,060	0,545	0,000	0,097	0,083	46,09	98,90	0,55
2	5,53	2,65	62,13	0,02	7,11	28,09	0,087	0,489	0,000	0,062	0,125	66,83	99,81	0,09
3	8,30	2,83	59,17	0,02	4,96	33,02	0,093	0,464	0,000	0,044	0,145	76,57	99,84	0,08
4	11,06	3,16	57,19	0,02	3,67	35,96	0,103	0,447	0,000	0,033	0,157	82,46	99,85	0,07
5	13,83	3,16	56,26	0,02	2,74	37,81	0,103	0,439	0,000	0,025	0,164	86,69	99,86	0,07
6	16,59	2,87	55,03	0,02	2,36	39,73	0,094	0,429	0,000	0,022	0,171	88,75	99,86	0,07
7	19,36	2,96	54,66	0,02	1,99	40,37	0,097	0,425	0,000	0,018	0,173	90,44	99,87	0,07
8	22,12	2,76	54,82	0,02	1,56	40,84	0,091	0,427	0,000	0,015	0,175	92,35	99,87	0,07

Table 32. Data corresponding to Screening Experiment 4.

Screening Exp. 5		**T**	**80 ºC**	**m$_{BuOH}$**	42,02 g	**n$_{BuOH}$**	0,567 mol
		R$_{BuOH/LA}$	**3**	**m$_{LA}$**	21,82 g	**n$_{LA}$**	0,188 mol
Catalyst	**CT-224**	**m$_{cat}$**	**0,544 g**	**m$_{H2O}$**	0,66 g	**n$_{H2O}$**	0,036 mol

t	$\dfrac{w \cdot t}{n_{LA}^{o}}$	AREA (%)					n$_j$ (mol)					X$_{LA}$ (%)	SELECTIVITY	
		H$_2$O	BuOH	DBE	LA	BL	H$_2$O	BuOH	DBE	LA	BL		S$_{BuOH}^{BL}$	S$_{BuOH}^{DBE}$
0	0,00	1,37	78,20	0,12	15,79	4,52	0,047	0,633	0,001	0,125	0,022	14,71	93,76	3,12
2	5,79	2,70	63,93	0,08	8,34	24,95	0,089	0,506	0,000	0,072	0,112	60,95	99,19	0,41
3	8,68	3,05	61,34	0,04	6,00	29,57	0,100	0,484	0,000	0,053	0,131	71,19	99,65	0,18
4	11,58	3,08	59,09	0,02	4,73	33,09	0,101	0,464	0,000	0,043	0,146	77,39	99,84	0,08
6	17,37	3,49	57,75	0,04	2,37	36,35	0,114	0,453	0,000	0,022	0,158	87,89	99,68	0,16
7	20,26	2,88	56,28	0,02	2,29	38,53	0,095	0,440	0,000	0,021	0,167	88,74	99,86	0,07
8	23,16	3,04	55,95	0,02	1,89	39,10	0,100	0,437	0,000	0,018	0,169	90,60	99,86	0,07

Table 33. Data corresponding to Screening Experiment 5.

Screening Exp. 6		**T**	**80 ºC**	**m$_{BuOH}$**	41,39 g	**n$_{BuOH}$**	0,558 mol
		R$_{BuOH/LA}$	**3**	**m$_{LA}$**	22,13 g	**n$_{LA}$**	0,191 mol
Catalyst	**Amberlyst 70**	**m$_{cat}$**	**0,534 g**	**m$_{H2O}$**	0,66 g	**n$_{H2O}$**	0,037 mol

t	$\dfrac{w \cdot t}{n_{LA}^{o}}$	AREA (%)					n$_j$ (mol)					X$_{LA}$ (%)	SELECTIVITY	
		H$_2$O	BuOH	DBE	LA	BL	H$_2$O	BuOH	DBE	LA	BL		S$_{BuOH}^{BL}$	S$_{BuOH}^{DBE}$
0	0,00	0,78	76,86	0,13	17,57	4,67	0,028	0,618	0,001	0,135	0,022	14,04	93,86	3,07
1	2,80	1,76	71,29	0,10	14,50	12,35	0,059	0,568	0,001	0,116	0,057	33,08	98,00	1,00
2	5,60	2,34	66,94	0,06	11,82	18,84	0,077	0,530	0,000	0,098	0,086	46,80	99,23	0,39
3	8,41	2,69	64,53	0,06	9,86	22,87	0,088	0,509	0,000	0,083	0,103	55,31	99,33	0,33
4	11,21	2,58	62,41	0,06	8,21	26,74	0,085	0,490	0,000	0,071	0,119	62,79	99,42	0,29
5	14,01	3,03	60,59	0,06	7,06	29,25	0,099	0,475	0,000	0,062	0,129	67,78	99,47	0,27
6	16,81	2,68	59,67	0,04	5,43	32,18	0,088	0,467	0,000	0,048	0,141	74,57	99,67	0,17
7	19,62	3,14	58,24	0,04	4,71	33,86	0,102	0,455	0,000	0,042	0,148	77,83	99,69	0,16
8	22,42	3,28	57,33	0,02	4,00	35,37	0,107	0,447	0,000	0,036	0,154	81,03	99,85	0,07

Table 34. Data corresponding to Screening Experiment 6.

	Screening Exp. 7		T	80 ºC	m_{BuOH}	41,92 g	n_{BuOH}	0,566 mol
			$R_{BuOH/LA}$	3	m_{LA}	22,05 g	n_{LA}	0,190 mol
Catalyst	Dowex 50Wx2		m_{cat}	0,532 g	m_{H2O}	0,66 g	n_{H2O}	0,037 mol

t	$\dfrac{w \cdot t}{n_{LA}^o}$	AREA (%)					n_j (mol)					X_{LA} (%)	SELECTIVITY	
		H_2O	BuOH	DBE	LA	BL	H_2O	BuOH	DBE	LA	BL		S_{BuOH}^{BL}	S_{BuOH}^{DBE}
0	0,00	1,43	76,63	0,11	16,77	5,07	0,049	0,620	0,001	0,131	0,024	15,52	95,21	2,39
2	5,60	2,88	59,65	0,04	6,13	31,30	0,095	0,470	0,000	0,054	0,139	71,83	99,66	0,17
3	8,41	3,17	57,96	0,02	3,41	35,44	0,104	0,455	0,000	0,031	0,155	83,29	99,85	0,08
4	11,21	3,38	55,86	0,02	2,85	37,89	0,111	0,437	0,000	0,026	0,165	86,30	99,86	0,07
5	14,01	2,90	55,51	0,02	1,95	39,62	0,095	0,434	0,000	0,018	0,171	90,47	99,86	0,07
6	16,81	2,62	56,07	0,02	1,45	39,84	0,087	0,439	0,000	0,014	0,172	92,72	99,86	0,07
7	19,61	3,36	54,89	0,02	1,46	40,26	0,110	0,429	0,000	0,014	0,174	92,73	99,87	0,07
8	22,42	2,71	53,87	0,02	1,32	42,07	0,089	0,420	0,000	0,012	0,181	93,59	99,87	0,07

Table 35. Data corresponding to Screening Experiment 7.

	Screening Exp. 8		T	80 ºC	m_{BuOH}	41,85 g	n_{BuOH}	0,565 mol
			$R_{BuOH/LA}$	3	m_{LA}	22,95 g	n_{LA}	0,189 mol
Catalyst	Amberlyst 36		m_{cat}	0,529 g	m_{H2O}	0,66 g	n_{H2O}	0,037 mol

t	$\dfrac{w \cdot t}{n_{LA}^o}$	AREA (%)					n_j (mol)					X_{LA} (%)	SELECTIVITY	
		H_2O	BuOH	DBE	LA	BL	H_2O	BuOH	DBE	LA	BL		S_{BuOH}^{BL}	S_{BuOH}^{DBE}
0	0,00	1,43	76,77	0,10	16,76	4,95	0,049	0,620	0,001	0,131	0,024	15,22	95,41	2,29
1	2,80	1,66	72,95	0,08	14,84	10,46	0,056	0,585	0,000	0,119	0,049	29,22	98,11	0,95
2	5,60	2,21	70,76	0,10	10,35	16,59	0,073	0,566	0,001	0,087	0,076	46,66	98,57	0,71
3	8,39	2,41	65,91	0,06	9,94	21,69	0,080	0,523	0,000	0,084	0,099	53,89	99,29	0,35
4	11,19	2,59	62,12	0,06	9,23	26,00	0,085	0,490	0,000	0,079	0,117	59,67	99,41	0,30
5	13,99	2,81	62,17	0,04	7,04	27,94	0,092	0,490	0,000	0,062	0,125	66,91	99,63	0,19
6	16,79	2,96	60,70	0,02	6,37	29,94	0,097	0,478	0,000	0,056	0,133	70,26	99,83	0,09
7	19,59	3,28	61,29	0,10	4,34	30,98	0,107	0,483	0,001	0,039	0,137	77,77	99,19	0,40
8	22,39	3,01	58,45	0,06	4,62	33,86	0,099	0,458	0,000	0,042	0,149	78,14	99,53	0,23

Table 36. Data corresponding to Screening Experiment 8.

Screening Exp. 9			T	80 ºC	m_{BuOH}	42,25 g	n_{BuOH}	0,570 mol
			$R_{BuOH/LA}$	3	m_{LA}	21,84 g	n_{LA}	0,188 mol
Catalyst	Amberlyst 35		m_{cat}	0,551 g	m_{H2O}	0,66 g	n_{H2O}	0,037 mol

t	$\dfrac{w \cdot t}{n_{LA}^{o}}$	AREA (%)					n_j (mol)					X_{LA} (%)	SELECTIVITY	
		H_2O	BuOH	DBE	LA	BL	H_2O	BuOH	DBE	LA	BL		S_{BuOH}^{BL}	S_{BuOH}^{DBE}
0	0,00	1,36	77,14	0,13	16,08	5,30	0,047	0,626	0,001	0,127	0,025	16,57	94,59	2,71
2	5,86	1,88	70,05	0,06	12,68	15,33	0,063	0,562	0,000	0,105	0,071	40,52	99,01	0,49
3	8,79	2,44	67,62	0,08	10,71	19,15	0,081	0,540	0,000	0,090	0,088	49,33	98,99	0,51
4	11,72	2,51	65,84	0,06	9,59	22,01	0,083	0,525	0,000	0,082	0,100	55,04	99,30	0,35
5	14,65	2,43	64,93	0,04	8,34	24,26	0,081	0,517	0,000	0,072	0,110	60,33	99,58	0,21
6	17,58	2,53	63,01	0,06	7,84	26,57	0,084	0,500	0,000	0,068	0,120	63,64	99,42	0,29
7	20,51	2,84	62,66	0,04	6,80	27,65	0,094	0,497	0,000	0,060	0,124	67,42	99,63	0,19
8	23,44	2,58	61,38	0,02	6,14	29,88	0,085	0,486	0,000	0,055	0,133	70,93	99,82	0,09

Table 37. Data corresponding to Screening Experiment 9.

Screening Exp. 10			T	80 ºC	m_{BuOH}	40,99 g	n_{BuOH}	0,553 mol
			$R_{BuOH/LA}$	3	m_{LA}	21,77 g	n_{LA}	0,187 mol
Catalyst	Amberlyst 46		m_{cat}	0,539 g	m_{H2O}	0,65 g	n_{H2O}	0,036 mol

t	$\dfrac{w \cdot t}{n_{LA}^{o}}$	AREA (%)					n_j (mol)					X_{LA} (%)	SELECTIVITY	
		H_2O	BuOH	DBE	LA	BL	H_2O	BuOH	DBE	LA	BL		S_{BuOH}^{BL}	S_{BuOH}^{DBE}
0	0,00	1,30	79,04	0,11	16,42	3,13	0,044	0,630	0,001	0,127	0,015	10,41	92,51	3,74
1	2,88	1,49	74,75	0,10	15,90	7,76	0,050	0,592	0,001	0,124	0,036	22,57	96,89	1,56
3	8,63	2,05	69,29	0,10	13,69	14,86	0,067	0,544	0,001	0,109	0,068	38,24	98,34	0,83
4	11,50	2,11	69,96	0,00	11,04	16,89	0,069	0,550	0,000	0,091	0,076	45,70	100,00	0,00
5	14,38	2,36	66,44	0,06	10,66	20,48	0,077	0,519	0,000	0,088	0,092	51,01	99,26	0,37
6	17,25	2,84	63,85	0,06	10,26	22,99	0,092	0,497	0,000	0,085	0,102	54,57	99,37	0,32
7	20,13	2,77	63,51	0,04	8,44	25,23	0,090	0,494	0,000	0,072	0,112	60,92	99,60	0,20
8	23,00	2,80	62,32	0,06	8,16	26,67	0,090	0,484	0,000	0,069	0,117	62,87	99,44	0,28

Table 38. Data corresponding to Screening Experiment 10.

Screening Exp. 11		T	80 ºC	m_{BuOH}	41,57 g	n_{BuOH}	0,561 mol
		$R_{BuOH/LA}$	3	m_{LA}	22,35 g	n_{LA}	0,192 mol
Catalyst	Amberlyst 15	m_{cat}	0,511 g	m_{H2O}	0,66 g	n_{H2O}	0,037 mol

t	$\dfrac{w \cdot t}{n_{LA}^o}$	AREA (%)					n_j (mol)					X_{LA} (%)	SELECTIVITY	
		H_2O	BuOH	DBE	LA	BL	H_2O	BuOH	DBE	LA	BL		S_{BuOH}^{BL}	S_{BuOH}^{DBE}
0	0,00	1,35	77,27	0,12	17,34	3,91	0,047	0,625	0,001	0,135	0,019	12,18	92,85	3,58
1	2,65	1,70	71,95	0,10	15,86	10,39	0,057	0,578	0,001	0,126	0,049	27,98	97,67	1,17
2	5,31	2,01	68,61	0,10	13,72	15,57	0,067	0,548	0,001	0,111	0,072	39,26	98,42	0,79
4	10,62	2,46	64,70	0,04	10,70	22,10	0,082	0,514	0,000	0,090	0,100	52,73	99,54	0,23
5	13,27	2,66	63,39	0,06	9,45	24,44	0,088	0,502	0,000	0,081	0,110	57,77	99,38	0,31
6	15,93	2,57	62,00	0,04	8,24	27,15	0,085	0,490	0,000	0,071	0,122	63,04	99,62	0,19
7	18,58	2,93	60,71	0,06	7,48	28,82	0,096	0,479	0,000	0,065	0,129	66,30	99,47	0,27
8	21,24	2,78	60,02	0,04	6,64	30,51	0,092	0,473	0,000	0,059	0,135	69,82	99,66	0,17

Table 39. Data corresponding to Screening Experiment 11.

Screening Exp. 12		T	80 ºC	m_{BuOH}	41,14 g	n_{BuOH}	0,555 mol
		$R_{BuOH/LA}$	3	m_{LA}	21,77 g	n_{LA}	0,187 mol
Catalyst	Amberlyst 16	m_{cat}	0,522 g	m_{H2O}	0,65 g	n_{H2O}	0,036 mol

t	$\dfrac{w \cdot t}{n_{LA}^o}$	AREA (%)					n_j (mol)					X_{LA} (%)	SELECTIVITY	
		H_2O	BuOH	DBE	LA	BL	H_2O	BuOH	DBE	LA	BL		S_{BuOH}^{BL}	S_{BuOH}^{DBE}
0	0,00	1,14	79,46	0,09	14,86	4,45	0,039	0,635	0,000	0,117	0,021	15,13	95,51	2,25
1	2,78	1,35	73,68	0,08	14,05	10,84	0,046	0,584	0,000	0,112	0,050	30,88	98,12	0,94
2	5,57	1,89	69,84	0,08	12,53	15,66	0,063	0,550	0,000	0,102	0,071	41,24	98,72	0,64
3	8,35	1,97	67,26	0,08	11,37	19,33	0,065	0,527	0,000	0,093	0,087	48,24	98,96	0,52
4	11,14	2,54	65,45	0,04	9,51	22,46	0,083	0,512	0,000	0,080	0,100	55,68	99,55	0,23
5	13,92	2,66	63,89	0,04	8,00	25,41	0,086	0,498	0,000	0,068	0,113	62,23	99,60	0,20
6	16,71	3,35	60,57	0,04	7,41	28,63	0,108	0,470	0,000	0,064	0,126	66,35	99,66	0,17
7	19,49	3,52	59,20	0,06	6,50	30,73	0,113	0,458	0,000	0,056		70,38	99,52	0,24
8	22,28	3,52	58,44	0,04	5,40	32,60	0,113	0,452	0,000	0,047		74,89	99,69	0,16

Table 40. Data corresponding to Screening Experiment 12.